

Effect of Broadband Radio Service Reallocation on 2900–3100 MHz Band Marine Radars: Base Station Unwanted Emissions

**Robert Achatz
Paul McKenna
Roger Dalke
Frank Sanders
John Carroll**



report series

Effect of Broadband Radio Service Reallocation on 2900–3100 MHz Band Marine Radars: Base Station Unwanted Emissions

**Robert Achatz
Paul McKenna
Roger Dalke
Frank Sanders
John Carroll**



U.S. DEPARTMENT OF COMMERCE

April 2015

DISCLAIMER

Certain commercial equipment and materials are identified in this report to specify adequately the technical aspects of the reported results. In no case does such identification imply recommendation or endorsement by the National Telecommunications and Information Administration, nor does it imply that the material or equipment identified is the best available for this purpose.

CONTENTS

List of Figures	vii
List of Tables	x
Acronyms	xi
Executive Summary	xv
1 Introduction.....	1
1.1 Previous Background Work.....	4
1.2 Report Organization.....	6
2 Unwanted Emissions.....	7
3 Method	9
4 Mathematical Foundation	13
4.1 Powers, Power Ratios, and IPC	13
4.2 Distance Separation with Spurious Attenuation	14
4.2.1 Constant SNR	14
4.2.2 Variable SNR	15
4.3 Distance Separation with FDR	16
5 Results.....	18
5.1 Parameters.....	18
5.2 Interference Protection Criteria	18
5.3 Interference Power Distributions	20
5.4 Distance separation with spurious attenuation.....	21
5.4.1 Constant SNR	21
5.4.2 Variable SNR	23
5.4.3 Comparison of constant SNR to variable SNR results.....	25
5.5 Distance and frequency separation with FDR	27
6 Conclusion	30
7 Acknowledgements.....	32
8 References	33
Appendix A : Unwanted Signal Power	35
A.1 Basic Frequency Dependent Interference Model.....	35
A.2 Transmitted Unwanted Signal Power	36
A.3 Received Unwanted Signal Power	38
A.4 Received Unwanted Signal Power in Terms of the Transmitted Unwanted Signal Power	39
A.5 References	39

Appendix B : Fast Method For Computing Segmented, LogNormal- Distribution Integral.....	41
B.1 References	43
Appendix C : Rise in Noise Power	44
Appendix D : Emission Limits	45
D.1 ITU-R Spurious Emission Limit.....	45
D.2 ETSI Spectrum Emission Mask.....	46
D.3 References.....	47
Appendix E : Variable SNR Data Examples	48
Appendix F : WiMAX Measured PSD and Filtered PSD.....	51
F.1 PSD Measurement	51
F.2 Filtered PSD Measurement.....	51
F.3 References	53
Appendix G : Radar IF Filter Frequency Responses	54
G.1 References.....	55
Appendix H : Results For Other INR	56
H.1 Results for -9 dB INR	56
H.2 Results for -12 dB INR	58
Appendix I : Probability.....	60

LIST OF FIGURES

Figure 1. Marine radar slotted array antenna (white bar) mounted on motor which spins it.....	3
Figure 2. BRS base station.....	3
Figure 3. Radio spectrum from 2500 to 3700 MHz with current allocations for air traffic control (ATC), weather, marine, and various Department of Defense (DOD) radar services.	4
Figure 4. Physical layout showing a network of BRS base stations contributing to the interfering signal power. The interference can cause the radar to not detect the target. Antenna pattern attenuation is not represented in this figure.	6
Figure 5. ITU power spectral density domains.....	7
Figure 6. Interfering power spectral density (centered around f_i) unwanted emissions are within the radar detection IF bandwidth (inner dashed line). Radar is vulnerable to unwanted emissions.	8
Figure 7. Interfering power spectral density (centered around f_i) after transmitter filter mitigation. Radar is protected from unwanted emissions.	8
Figure 8. General block diagram of BRS transmitters and radar system. TX represents the transmitter, TF represents the transmitter filter, TX ANT represents the transmitter antenna, ANT represents the radar antenna, FEF represents the front-end filter, LNA represents the low-noise amplifier, IFF represents the IF filter, and DET represents the threshold detector.	8
Figure 9. Short radar to target ranges as in (a) and (b) are analyzed with a constant SNR while long radar to target ranges as in (c) are analyzed with a variable SNR.	11
Figure 10. RCS and range for 10 IEC 62388 standard clutter free test cases with pulse range limits. Short and long pulses are separated by solid blue line at 5.6 km. Medium pulse ranges are between dashed red lines at 1.4 and 22.2 km.....	12
Figure 11. Radar performance with GN interfering signal, Swerling 1 target, non-coherent integration performance, and baseline performance of $0.8 P_d$, $10^{-4} P_{fa}$. The long and short pulses were integrated 6 and 14 times, respectively.	19
Figure 12. Radar performance degradation with GN interfering signal, Swerling 1 target, non-coherent integration, and baseline performance of $0.8 P_d$, $10^{-4} P_{fa}$. The long and short pulses were integrated 6 and 14 times, respectively.	20
Figure 13. INR distributions at various distances to the closest base station when there is 60 dB spurious attenuation.....	21
Figure 14. Separation distance versus reliability for -6 dB INR. 95 dB attenuation produces separation distances less than the 1 km propagation model limit and is not shown.	22

Figure 15. SNR distributions for 10 IEC 62388 standard clutter free test cases with power margin removed. Only seven curves are visible because cases 2 and 5, 6 and 7, and 8 and 9 have similar target parameters.....	24
Figure 16. INR distributions for 10 IEC 62388 clutter free test cases with spurious attenuation set to 60 dB. The separation distance between the radar and the closest base station is set to the radar to target range plus a 1 km base station to target distance. Only seven curves are visible because cases 2 and 5, 6 and 7, and 8 and 9 have similar target distances.	24
Figure 17. Comparison of constant and variable SNR results for -6 dB INR and 90% reliability.	26
Figure 18. Measured PSD, filtered measured PSD, and SEM.....	28
Figure 19. FDR for ideal short pulse, 20 MHz bandwidth, IF filter.	28
Figure 20. Separation distance versus frequency separation for 50 and 90% reliability with short pulse 20 MHz radar detection IF bandwidth when INR is -6 dB.....	29
Figure A-1. Basic interference model. TX represents the transmitter source, TX Filter represents the transmitter filter, ANT represents the antenna, and RX filter represents the receiver filter.	35
Figure A-2. Hypothetical PSD with ITU domains.....	36
Figure C-1. Rise in noise power relative to receiver noise power for interfering signal with Gaussian noise characteristics.	44
Figure D-1. 3GPP spectrum emission mask in 30.0 kHz bandwidth.....	47
Figure E-1. Case 1 reliability as a function of separation distance. The thick vertical black line at 38.0 km is the separation distance used in our analysis. Reliabilities for spurious attenuations above 85 dB are approximately 1.0 for all separation distances.....	48
Figure E-2. Case 6 reliability as a function of separation distance. The thick vertical black line at 7.8 km is the separation distance used in our analysis. Reliabilities for spurious attenuations above 90 dB are approximately 1.0 for all separation distances.....	49
Figure E-3. Case 1 reliability as a function of radar to target range. The thick vertical black line at 37.0 km is the radar to target range used in our analysis. All spurious attenuation curves lie on top of each other.....	49
Figure E-4. Case 6 reliability as a function of radar to target range. The thick vertical black line at 6.8 km is the radar to target range used in our analysis. Spurious attenuation curves from 80 to 105 lie on top of each other. Reliability anomalies from 1 to 2 km are due to numerical integration error.....	50
Figure F-1. PSD measurement.....	51
Figure F-2. Transmitter filter frequency response.	52

Figure F-3. Measured and filtered PSDs.....	53
Figure G-1. Radar A measured and ideal, long and short pulse IF filter frequency responses.	54
Figure G-2. Radar C measured and ideal, long and short pulse IF filter frequency responses.....	55
Figure H-1. Separation distance versus reliability for -9 dB INR. 95 dB attenuation produces separation distances less than the 1 km propagation model limit and is not shown.	56
Figure H-2. Spurious attenuation for IEC 62388 standard clutter free test cases with -9 dB INR using constant and variable SNR for 90% reliability.	57
Figure H-3. Separation distance versus frequency separation for 50 and 90% reliability -9 dB INR with 20 MHz radar detection IF bandwidth.	57
Figure H-4. Separation distance versus reliability for -12 dB INR.	58
Figure H-5. Spurious attenuation for IEC 62388 standard clutter free test cases with -12 dB INR using constant and variable SNR for 90% reliability.	59
Figure H-6. Separation distance versus frequency separation for 50 and 90% reliability -12 dB INR with 20 MHz radar detection IF bandwidth.	59

LIST OF TABLES

Table 1. IEC 62388 standard clutter free test cases.	11
Table 2. Radar and BRS parameters used for analysis.	18
Table 3. Baseline ideal SNR for a 1.9 degree beam-width antenna at baseline performance 0.8 Pd and $10 - 4 Pfa$. PW is pulse width, PRF is pulse repetition frequency, BW is IF filter bandwidth, RR is rotation rate, and np is the number of pulses integrated.	18
Table 4. Relevant IPC parameters for baseline 0.8 Pd , $10^{-4} Pfa$ with long and short pulse widths. S, I, and N are evaluated at the receiver input.	20
Table 5. Analysis results for -6.0 dB allowable INR.	22
Table 6. Separation distances for all INR at 90% reliability.	23
Table 7. Spurious attenuation for IEC 62388 standard clutter free test cases for 90% reliability.	25
Table 8. Spurious attenuation for IEC 62388 standard clutter free test cases using constant SNR (C) and variable SNR (V) for 90% reliability. Case 1 difference is not available (NA) because the required spurious attenuation is below the minimum tested.	26
Table 9. Spurious attenuation, L_{spur} , FDR, L_{fdr} , and frequency separation, Δf , needed for 90% reliability for 20 MHz bandwidth short pulse at 1 km distance separation.	29
Table B-1. Probability, qk , and corresponding standard normal deviate, zk , for the each of the 26 segments in the aggregate distribution function.	42
Table D-1. ITU-R Spurious emission power limit for BRS base station.	46
Table D-2 Spectrum emission mask breakpoints.	46
Table F-1. Transmitter filter specifications.	52
Table H-1. Separation distance results for -9.0 dB allowable INR and 2.7% allowable degradation.	56
Table H-2. Separation distance results for -12.0 dB allowable INR and 1.4% allowable degradation.	58

ACRONYMS

3GPP	3 rd Generation Partnership Project
APD	Amplitude probability distribution
AWGN	Additive white Gaussian noise
BPF	Bandpass filter
BRS	Broadband radio service
BW	Bandwidth
CFAR	Constant false alarm rate
CW	Continuous wave
dB	Decibel
dB_i	Decibels relative to the gain of an isotropic antenna
dB_m	Decibels relative to a milliwatt
dB_{sm}	Decibels relative to a square meter
dBW	Decibels relative to a watt
DOD	Department of Defense
EIRP	Effective isotropic radiated power
ETSI	European Telecommunications Standards Institute
FDD	Frequency division duplex
FDR	Frequency dependent rejection
FE	Front-end
FEF	Front-end filter
FS	Free space
GHz	Gigahertz
GN	Gaussian noise
Hz	Hertz
IEC	International Electrotechnical Committee
IEEE	Institute of Electrical and Electronics Engineers

IF	Intermediate frequency
INR	Interference to noise power ratio
IPC	Interference protection criteria
ITM	Irregular terrain model
ITS	Institute for Telecommunication Sciences
ITU	International Telecommunication Union
ITU-R	ITU Radiocommunication Sector
km	Kilometer
kHz	kilohertz
LNA	Low-noise amplifier
LNFE	Low-noise front-end
LTE	Long Term Evolution
MHz	Megahertz
MIMO	Multiple-input multiple-output
MSC	Maritime Safety Committee
nmi	Nautical mile
ns	Nanosecond
NTIA	National Telecommunications and Information Administration
OFDM	Orthogonal frequency division multiplexing
OFDMA	Orthogonal frequency division multiple access
OOB	Out-of-band
PRF	Pulse repetition frequency
PRI	Pulse repetition interval
PSD	Power spectral density
RCS	Radar cross section
RF	Radio frequency
RPM	Revolutions per minute

SA	Spectrum analyzer
SEM	Spectrum emission mask
SINR	Signal to interference plus noise ratio
SNR	Signal to noise ratio
SOLAS	Safety of life at sea
STC	Sensitivity time control
TDD	Time division duplex
UMTS	Universal Mobile Telecommunications System
UN	United Nations
UN/MSC	United Nations Maritime Safety Committee
USCG	United States Coast Guard
VSA	Vector signal analyzer
WGN	White Gaussian noise
WiMAX	Worldwide interoperability for microwave access

EXECUTIVE SUMMARY

Spectrum reallocation is often necessary to accommodate new services which can potentially increase business productivity and enhance the lives of private citizens. However, reallocating services to bands near those used by incumbent services—or, in some cases, to those same bands—can cause interference to the incumbent service.

Spectrum reallocation can cause interference in radar systems in a number of ways. A system reallocated to a nearby band can introduce unwanted signals into the radar detection bandwidth. Also, a system reallocated to a nearby band can overload the radar receiver front-end and cause gain compression, increased noise power, and intermodulation in the radar detection bandwidth.

The U.S. Coast Guard (USCG) asked the National Telecommunications and Information Administration Institute for Telecommunication Sciences (NTIA/ITS) to investigate effects of reallocation on the 2900–3100 MHz band marine radar service by determining interference protection criteria (IPC) and analyzing strategies for mitigating the interference.

Here we investigate the effects of reallocation to accommodate the broadband radio services (BRS) on the 2900–3100 MHz band marine radar service. The BRS is the next generation of personal communications services which will provide wideband Internet communications to mobile users. Results of our investigations have been assembled into three reports subtitled “Background,” “Unwanted Emissions,” and “Front-end Overload.”

This report analyzes the effect of unwanted emissions from a broadband radio service (BRS) base station on magnetron radar receiver performance. This report builds upon the interference model developed in the previous background report where we demonstrated that unwanted emissions were Gaussian distributed and aggregated. Results include distance separation and frequency separation that meet IPC. Baseline radar system performance was set at a 0.8 probability of detection and 10^{-4} probability of false alarm. Interference to noise ratios (INR) of -6, -9, and -12 dB were investigated.

Distance separation was computed from expressions for radar link reliability. Reliability in this context is dependent solely on radio wave propagation path loss variability. So that anomalous radio wave propagation ducting conditions do not influence results, 90% reliability is used. Two expressions for reliability were provided. One expression assumed constant radar signal to noise ratio (SNR) corresponding to short radar to target ranges. This method does not require knowing the radar to target link budget.

The other expression assumed variable SNR which is valid over any radar to target range. This method requires complete knowledge of the radar to target link budget. We used targets from the IEC 62388 standard clutter free test cases to set radar to target link budget parameters. Base station to radar path length was set to the radar to target range plus 1 km.

The constant SNR case is important because it can be easily applied to the most demanding case where the ship with the radar is close to the target and the base station. The expression for variable SNR is the most general and useful for situations where close radar to base station distances are not likely.

Distance separation calculations for constant SNR showed that 90 dB spurious attenuation could provide 90% reliability at a separation distance of 1.2 km when INR is -6 dB. The separation distance decreased below 1 km with 95 dB spurious attenuation. For reference, the ETSI -52 dBm/MHz unwanted emissions limit outside the BRS operating band corresponds to 95 dB spurious attenuation.

Results for variable SNR agreed with those using constant SNR at short radar to target ranges. However, as radar to target range increased, less spurious attenuation was needed. The largest difference was with case 4, a SOLAS ship 21.4 km away from the radar, where 7.1 dB less spurious attenuation was needed when INR is -6 dB. Consequently the constant SNR reliability expression can be considered worst case.

We also showed how frequency separation could be computed by replacing spurious attenuation by an expression for FDR. The FDR were calculated from measured PSD, filtered PSD, spectrum emission mask, and idealized IF filter frequency responses that corresponded with measured filter frequency responses. SNR was assumed to be constant so results are worst case. The results showed that 90 % reliability IPC could be met at 1.2 km separation distance with 92.8 MHz and 99.7 MHz for the filtered PSD and SEM when INR is -6 dB. We found that filtered PSD frequency separation can be reduced from 92.8 MHz to 54.6 MHz when the distance separation is increased to 32.8 km.

Results for the -9 dB and -12 dB INR cases differed in most cases. For example, the separation distance for the constant SNR case increased to 1.7 and 2.7 km with 90 dB spurious attenuation for INR of -9 and -12 dB, respectively. For variable SNR, case 4 required 8.7 and 11.2 dB less spurious attenuation than constant SNR for INR of -9 and -12 dB, respectively. Frequency separation did not increase when the INR was decreased to -9. However it did increase to 99.3 MHz when INR was decreased to -12 dB.

The results in this report are encumbered with two caveats. First, the results are for a frequency division duplexing (FDD) BRS base station signal that occupies one 10 MHz BRS channel. Results need to be adjusted to accommodate more channels. Second, these results are based on magnetron radar signal processing. Additional analysis is needed to assess the impact to solid-state radar receivers because their signal processing is very different from that in the magnetron radar receiver. The signal processing affects receiver sensitivity and IF selectivity and estimates of separation distance and frequency separation need to take this into account.

EFFECT OF BROADBAND RADIO SERVICE REALLOCATION ON 2900–3100 BAND MARINE RADARS: BASE STATION UNWANTED EMISSIONS

Robert Achatz, Paul McKenna, Roger Dalke, Frank Sanders, John Carroll¹

Spectrum reallocations may place broadband radio services (BRS) near spectrum used by 2900–3100 MHz band marine radars. Signals from the BRS base stations can potentially introduce unwanted emissions in the radar detection bandwidth and cause interference. Interference protection criteria (IPC) are needed to mitigate this effect. The primary IPC of concern are the interference to noise power ratio (INR) and the reliability of the radar link at a specified radar signal to noise power ratio (SNR). Reliability is determined by radio wave propagation path loss variability which increases with distance. Distance separation between base stations and radar for various spurious attenuations were calculated using reliability expressions for short radar to target ranges with constant SNR and for longer radar to target ranges with variable SNR. For a magnetron radar under clutter free conditions, 90 dB of spurious attenuation is needed to obtain 90% radar operational reliability at 1.2 km when the INR is -6 dB and the SNR is constant. Reducing the INR to -9 and -12 dB increased the separation distance to 1.7 and 2.7 km, respectively. At longer base station to radar separation distances, variable SNR required less spurious attenuation than constant SNR. Consequently, constant SNR analysis can be considered worst case. Distance and frequency separation were calculated using frequency dependent rejection (FDR). These calculations showed that for constant SNR 92.8 MHz of frequency separation is required to meet the 90% reliability IPC at 1.2 km separation distance when the INR is -6 dB. Only 54.6 MHz frequency separation is needed when the separation distance is increased to 32.8 km.

Keywords: broadband radio service, frequency dependent rejection, interference, interference protection criteria, marine radar, radar, radio wave propagation, radio spectrum engineering, spurious emissions, unwanted emissions

1 INTRODUCTION

Spectrum reallocation is often necessary to accommodate new services which can potentially increase business productivity and enhance the lives of private citizens. However, reallocating services to bands near those used by incumbent services—or, in some cases, to those same bands—can cause interference to the incumbent service.

Spectrum reallocation can cause interference in radar systems in a number of ways [1], [2], [3], [4]. For example, a system moved to a nearby band can introduce unwanted emissions into the radar detection bandwidth. Also, emissions from a system reallocated to a nearby band can overload the radar receiver front-end (receiver circuits operating at the carrier frequency) and cause gain compression, increased noise power, and intermodulation in the radar detection bandwidth.

¹The authors are with the Institute for Telecommunication Sciences, National Telecommunications and Information Administration, U.S. Department of Commerce, Boulder, CO 80305.

The U.S. Coast Guard (USCG) asked the National Telecommunications and Information Administration Institute for Telecommunication Sciences (NTIA/ITS) to investigate effects of spectrum reallocation on the 2900–3100 MHz band marine radar service by determining interference protection criteria (IPC) and analyzing strategies for mitigating the interference.

Results of these investigations are expected to be useful to regulatory and standards bodies which are responsible for developing IPC including the NTIA [5]; the International Telecommunication Union (ITU) [6]; the International Electrotechnical Commission (IEC) [7], which is currently devising IPC tests on behalf of the United Nations Maritime Safety Committee (UN/MSC) [8]; and the Institute of Electrical and Electronics Engineers (IEEE) [9].

In this series of reports we analyze the effects of reallocation to accommodate broadband radio services (BRS) on the 2900–3100 MHz band marine radar service. The BRS is the next generation of personal communications services which will provide wideband Internet communications to mobile users. Spectrum regulators are currently investigating various reallocation strategies to accommodate BRS growth.

Marine radars are used by ships to avoid collisions with objects while traveling in oceans, seas, lakes, and rivers. An example of a marine radar antenna mounted on a ship is shown in Figure 1. Detection of objects, referred to as targets, is often difficult. Even on calm seas, the target can have significant radar cross section (RCS) variation and corresponding reductions in signal power. The target can also be obscured by signal reflections or clutter from waves and precipitation.

These 2900–3100 MHz band radars are often referred to as S-band marine radars. Similar radars that operate in the 9200–9500 MHz band are often referred to as X-band marine radars. The primary advantage of S-band radar signals is that they have less precipitation attenuation than X-band radar signals. This allows S-band radars to detect smaller objects at longer distances in adverse weather conditions. Large ships subject to international safety of life at sea (SOLAS) regulations generally operate with radars in both bands.

BRS providers promise to deliver fast, reliable Internet service to users wherever they are. An example of a BRS base station is shown in Figure 2. Potential unwanted emissions and front-end overload problems in 2900–3100 MHz band marine radars from BRS base stations were brought to the attention of the International Telecommunication Union in November 2009 by the United Kingdom [10].

Significant amounts of spectrum are needed for widespread BRS use. BRS systems are already operating in the 2500–2690 MHz band. The 3500–3650 MHz band has been evaluated for reallocation [11]. Other reallocations in the 2700–3700 band, currently allocated to a number of radar services as shown in Figure 3, could also affect 2900–3100 MHz band marine radars.

BRS and radar system characteristics are derived from those used by internationally recognized groups. The BRS system is modeled after systems devised by the European Technical Standards Institute (ETSI) Universal Mobile Telecommunications System (UMTS) committee/3rd Generation Partnership Project (3GPP) [12], ITU [13], and the WiMAX Forum [14]. The radar

system is modeled after a system devised by the IEC 62388 standard shipborne radar committee [7] for industry acceptance testing.



Figure 1. Marine radar slotted array antenna (white bar) mounted on motor which spins it.

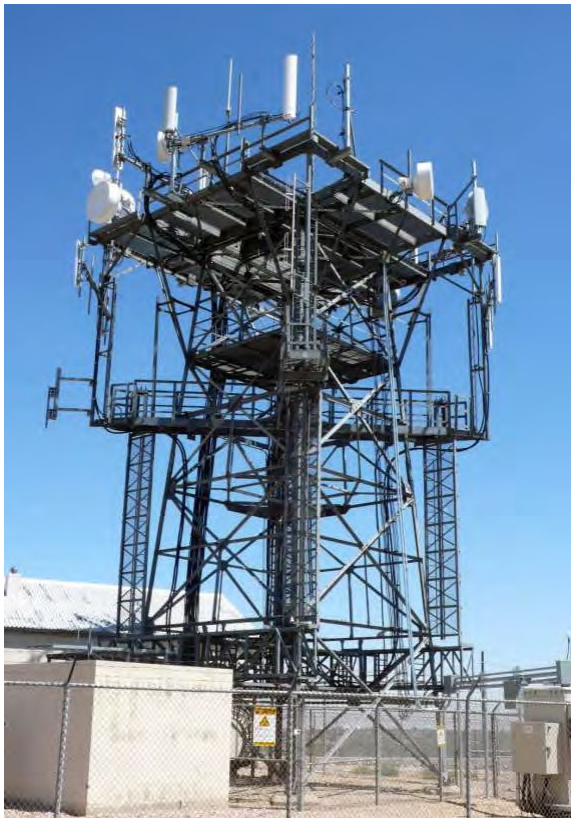


Figure 2. BRS base station.

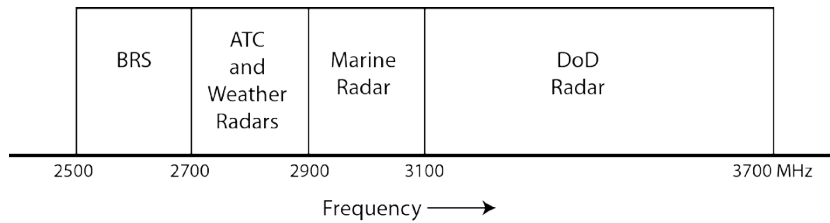


Figure 3. Radio spectrum from 2500 to 3700 MHz with current allocations for air traffic control (ATC), weather, marine, and various Department of Defense (DOD) radar services.

1.1 Previous Background Work

The IPC, scenario, and models needed for interference analysis are provided in the previous background report [15] and briefly summarized here. IPC are needed to reduce the probability of collision while not placing onerous burdens on other systems using the radio spectrum. Our objective is to determine IPC and factors such as distance and frequency separation that can mitigate the effects of the interfering signal so IPC can be met. IPC for base station interference in the marine radar receiver include:

- Radar baseline performance level, signal to noise ratio (SNR), and reliability
- Radar allowable degraded performance level, interference power level, and reliability

The physical scenario used for interference analysis is shown in Figure 4. We assume a radar target is located between a network of BRS base stations and a ship with a 2900–3100 MHz band magnetron marine radar. Weather conditions are assumed to be benign so that there is no signal “clutter” from reflections off precipitation or waves.

Radar targets include shorelines, ships, boats, and navigational buoys. The target RCS, which varies or fluctuates with time, is modeled with a statistical distribution. The mean of the distribution is dependent on target aspect angle, shape, and materials.

The base stations are modeled after those described by ETSI UMTS, 3GPP, ITU, and WiMAX groups. BRS signals use orthogonal frequency division multiple access (OFDMA) and are transmitted within BRS channels characterized by their center frequency and bandwidth. Transmit and receive signals use frequency division duplexing (FDD) so that transmissions can occur at all times. The signals are transmitted from antennas that typically cover 60 degree azimuth sectors with slant, 45 degree polarization. Although more than one BRS channel can be transmitted from the same antenna, we assume only one 10 MHz BRS channel is transmitted.

The radar is modeled after the magnetron radar in the IEC 62388 standard for shipborne radars. The radar transmits periodic pulses from a rotating antenna with a narrow antenna beam width and horizontal polarization. Typically short, medium, and long pulse widths are used to detect targets at different ranges and range resolution. Pulses arriving within the time it takes the antenna to traverse its beam width are integrated to enhance SNR.

The interfering radio wave propagation path is the path from the base station to the radar. The desired propagation path is the path from the radar to the target and back to the radar. These paths can have path loss variation depending on atmospheric conditions, which produces power fading and enhancement. Path loss variability occurs at longer distances from hour to hour and is characterized with a statistical distribution. The ITS Irregular Terrain Model (ITM) radio wave propagation model is used because it is able to predict power fading and enhancement caused by path loss variability.

Besides establishing IPC, scenario, and models, the previous background report addressed three fundamental interference analysis issues including

- **BRS signal characteristics:** BRS emissions from a single base station can be reasonably modeled with Gaussian noise. Since its statistics are Gaussian it follows that emissions from an aggregate of base stations will also be Gaussian.
- **Aggregate interfering emissions:** The interfering signal is the sum of signals from an aggregate of base stations, the mean power and distribution of the aggregate emissions can be determined using ITM and Monte Carlo analysis, and the aggregate emissions from 10 base stations spaced 3 km apart could have as much as 6 dB more power at some distances as compared to a single base station.
- **Variable SNR:** Interference analysis for scenarios with long radar to target ranges need to account for a variable radar SNR caused by atmospheric conditions that vary from hour to hour. While devising a method for incorporating variable SNR we found that there was a considerable amount of excess power in radar to target link budgets used in acceptance tests. Although this excess SNR could potentially mitigate interference we found that it is needed to accommodate reductions in target mean RCS due to different target aspects, shapes, and materials. We recommended removing the excess power prior to interference analysis by reducing the mean RCS.

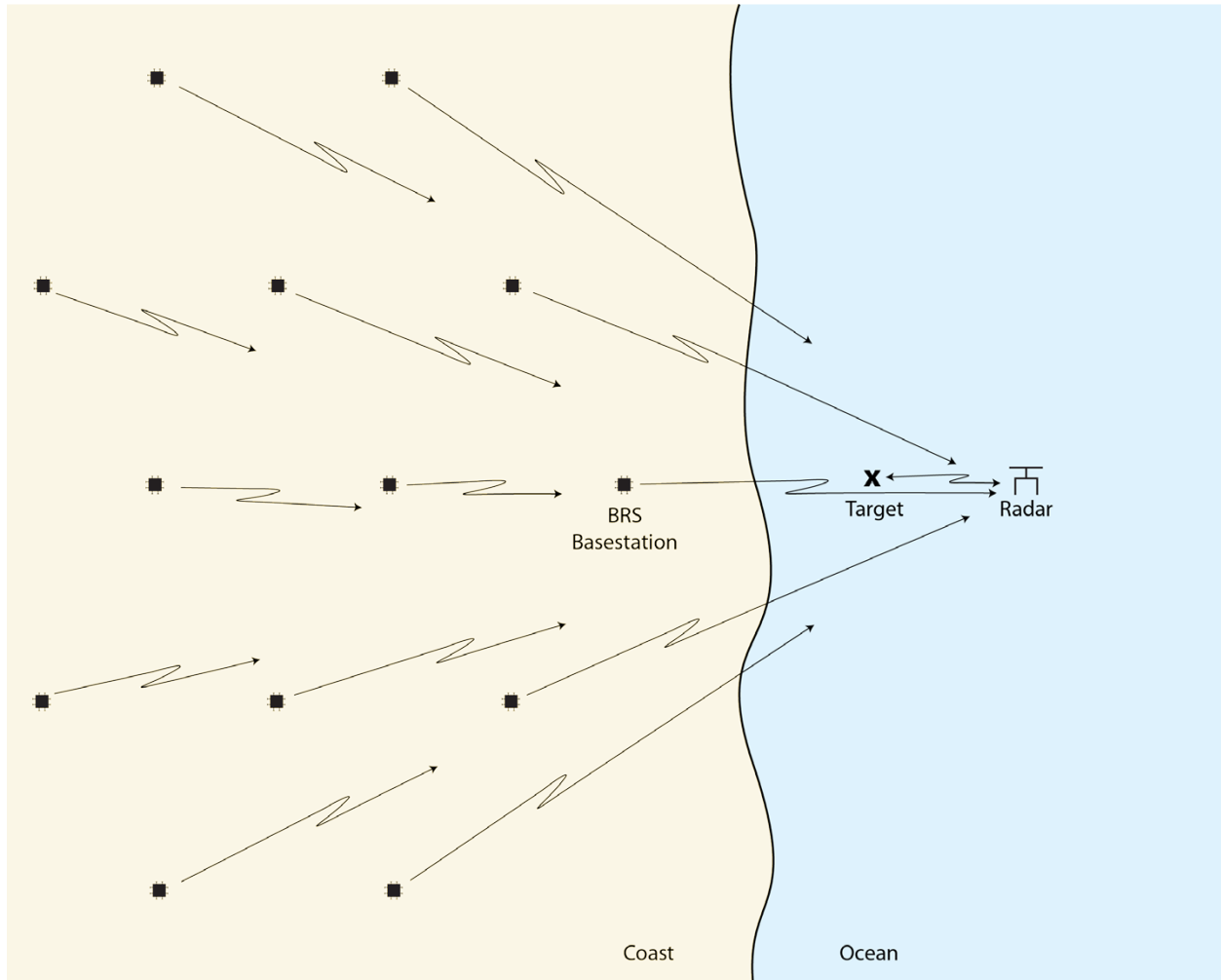


Figure 4. Physical layout showing a network of BRS base stations contributing to the interfering signal power. The interference can cause the radar to not detect the target. Antenna pattern attenuation is not represented in this figure.

1.2 Report Organization

This report determines allowable INR IPC and the distance and frequency separations needed to meet the allowable IPC. Distance separation is analyzed with constant and variable SNRs corresponding to short and long radar to target ranges, respectively. Results are compared to determine worst case conditions. Frequency separation is analyzed using frequency dependent rejection (FDR) which takes the transmitted power spectral density (PSD) and the radar receiver IF filter frequency responses into account. We also show how interference can be mitigated by the combination of distance and frequency separation. The general problem is discussed Section 2. Our approach to solving the problem is provided in Section 3. A mathematical description of the method is given in Section 4. Results are provided in Section 5. The Appendices provide additional information for the interested reader.

2 UNWANTED EMISSIONS

Unwanted emissions are precisely defined by the ITU-R [16], which recognizes three transmitted signal power spectral density (PSD) domains referred to as necessary bandwidth, out-of-band (OOB), and spurious. Collectively, OOB and spurious emissions are referred to as unwanted emissions. Figure 5 illustrates these domains.

In general the OOB domain begins at the edge of the necessary bandwidth and ends at ± 2.5 times the necessary bandwidth from the transmitter center frequency. The spurious domain follows the OOB domain. The necessary bandwidth contains most of the modulated signal power, the spurious region contains unwanted signals incidental to transmission, and the OOB region between them contains both modulated and incidental signals.

Effects of unwanted emissions are mitigated by decreasing transmitter power, increasing the distance separating the base stations from the radar, and increasing the frequency separation between base station and radar center frequencies.

Unwanted emissions can also be mitigated by transmitter filtering. An example of unwanted emissions before and after transmitter filtering is shown in Figures 6 and 7. As Figure 8 shows, the transmitter filter is located between the transmitter and the transmitter antenna. Although the IF filter in the radar signal processing block can attenuate unwanted emissions, it is constrained by its requirement to maximize radar signal power. Nevertheless, we will see that its design has a significant effect on frequency separation.

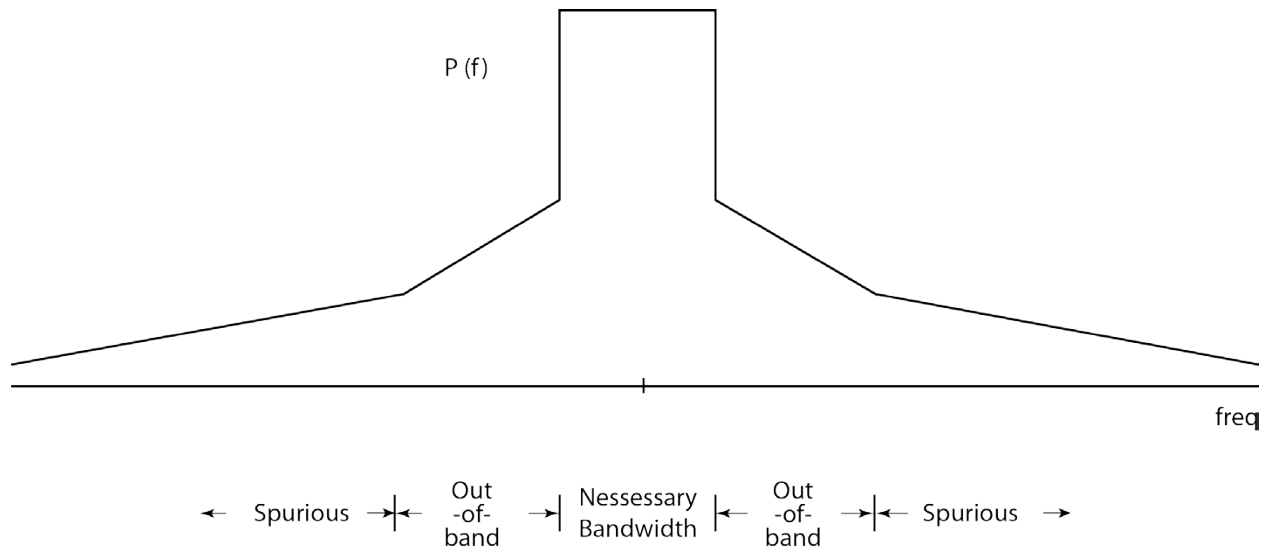


Figure 5. ITU power spectral density domains.

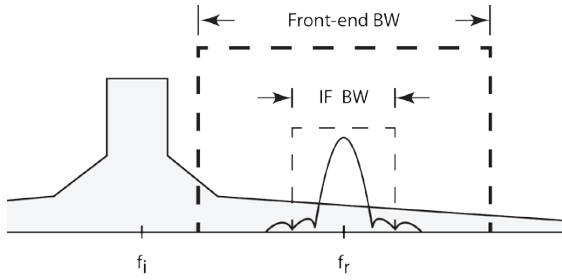


Figure 6. Interfering power spectral density (centered around f_i) unwanted emissions are within the radar detection IF bandwidth (inner dashed line). Radar is vulnerable to unwanted emissions.

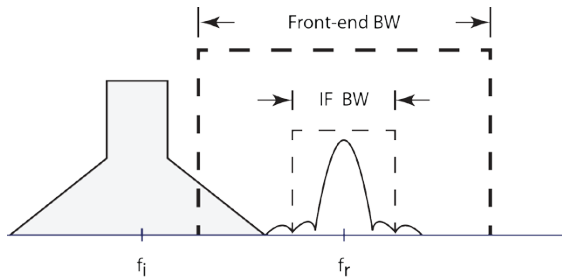


Figure 7. Interfering power spectral density (centered around f_i) after transmitter filter mitigation. Radar is protected from unwanted emissions.

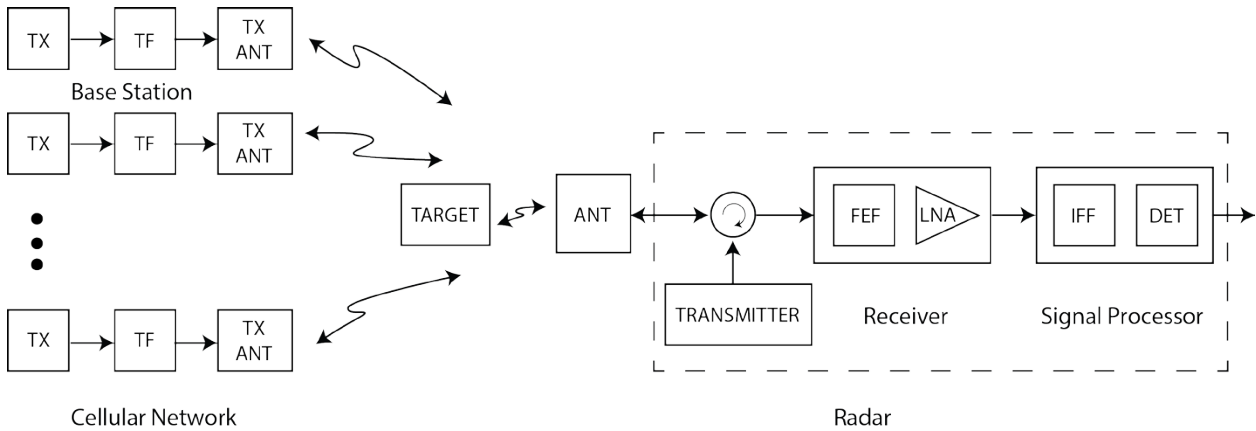


Figure 8. General block diagram of BRS transmitters and radar system. TX represents the transmitter, TF represents the transmitter filter, TX ANT represents the transmitter antenna, ANT represents the radar antenna, FEF represents the front-end filter, LNA represents the low-noise amplifier, IFF represents the IF filter, and DET represents the threshold detector.

3 METHOD

The previous background report [15] showed that the aggregate base station interference was Gaussian distributed. This finding is very advantageous because it allows us to repurpose theoretical expressions for predicting marine radar performance in Gaussian receiver noise for analyzing effects of aggregate base station unwanted emissions on marine radar receivers [17].

Consequently our analytic method establishes baseline SNR from baseline probability of detection, P_d , and probability of false alarm, P_{fa} . Allowable interference to noise ratio (INR) is then determined from the signal to interference plus noise ratio (SINR) corresponding to the allowable P_d and P_{fa} . Note that the unwanted emissions do not have to be “white” Gaussian noise with a constant PSD. This approach can be used even for unwanted OOB emissions where the PSD is not constant but sloped.

Having established the SNR and INR IPC, we proceed to determine distance and frequency separation with two methods that have distinctly different transmitter and receiver filtering assumptions. Our first method assumes that frequency separation places the unwanted emissions in the spurious domain and the spurious emission PSD is constant. Because the PSD is constant the emissions can be specified by one spurious attenuation parameter defined as

$$l_{spur} = \frac{p_{ta}}{\psi_{ref}} \quad (1)$$

where p_t is the total power at the transmit antenna input and ψ_{ref} is the spurious power measured in an ITU reference equivalent noise bandwidth, b_{ref} . More details regarding spurious attenuation can be found in Appendix A.

The second method replaces spurious attenuation with frequency dependent rejection (FDR). Frequency dependent rejection (FDR) is the fraction of transmitted power that is received at any frequency separation

$$\Delta f = f_t - f_r \quad (2)$$

where f_t and f_r are the transmitter center frequency and received frequency, respectively. FDR is computed from an actual PSD and IF filter frequency response

$$l_{fdr}(\Delta f) = \frac{\hat{p}_{ta}}{\int_{-\infty}^{\infty} \hat{p}_{ta}(f) |h_{if}(f + \Delta f)|^2 df} \quad (3)$$

where $\hat{p}_{ta}(f)$ is the BRS base station PSD at the transmit antenna input, $h_{if}(f)$ is the radar IF filter frequency response, and

$$\hat{p}_{ta} = \int_{-\infty}^{\infty} \hat{p}_{ta}(f) df \quad (4)$$

is the total power at the transmit antenna input.

Propagation path loss variability caused by atmospheric conditions further complicates our method. We address this by including radar link reliability in the separation distance calculation. In this context link reliability is determined solely by propagation path loss variability and is independent of electrical or mechanical malfunction. To avoid including the effects of radio wave propagation ducting we use a 90% reliability goal.

Reliability is included into the analysis in two ways. First, the interfering path from the base station to the radar is allowed to have path loss variability but the desired radar to target link is not. The underlying assumption in this approach is that the radar to target distance is short and SNR is constant. This is shown in Figures 9(a) and 9(b). With constant SNR only the aggregate interference power distribution is needed to compute reliability and separation distance.

The second way is to allow both interfering and desired path loss to vary. This is valid for any radar to target distance including the long radar to target range in Figure 9(c) where path loss and SNR variability can be high. With variable SNR, the radar power probability distribution is needed in addition to the aggregate interference distribution function to compute reliability and separation distance.

The radar power probability distribution is derived from targets given in the IEC 62388 standard. The set of targets, summarized in Table 1, is diverse in that it includes distributed targets such as shorelines, complex targets such as ships and boats, and point targets such as channel markers and buoys. The incongruity between the descriptive shoreline height and the height used in calculations is assumed to be due to terrain irregularity. Figure 10 displays the targets with respect to their RCS and range. Range limits for each pulse width based on manufacturer literature are also shown. The short pulse is limited to ranges up to 5.6 km (3 nmi) and the long pulse from 5.6 to 44.4 km (3 to 24 nmi). The medium pulse range from 1.4 to 22.2 km (0.75 to 12 nmi) overlaps short and long pulse ranges. The RCS of these targets are reduced to remove excess power needed to accommodate different target aspect angles, shapes, and materials by

$$\hat{\sigma}_{av} = \sigma_{av}/m \quad (5)$$

where σ_{av} is the mean RCS and m is the excess power margin.

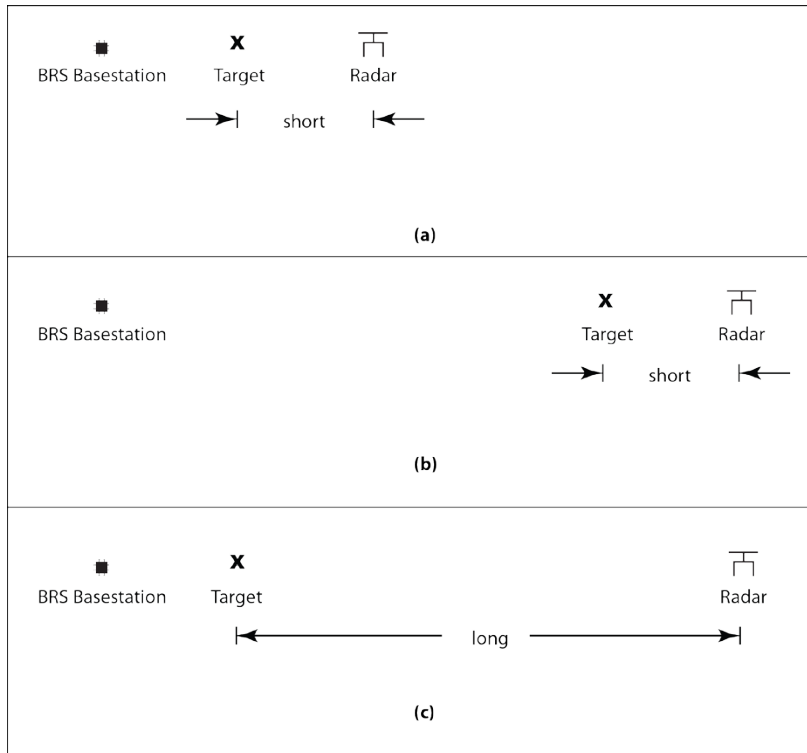


Figure 9. Short radar to target ranges as in (a) and (b) are analyzed with a constant SNR while long radar to target ranges as in (c) are analyzed with a variable SNR.

Table 1. IEC 62388 standard clutter free test cases.

Case	Target	Height (m)	Range		RCS (m ²)
			nmi	km	
1	60m high shoreline	50.0	20.0	37.0	50000.0
2	6 m high shoreline	5.0	8.0	14.8	5000.0
3	3 m high shoreline	2.5	6.0	11.1	2500.0
4	SOLAS ship > 5000gt	10.0	11.0	20.4	30000.0
5	SOLAS ship > 500gt	5.0	8.0	14.8	1000.0
6	Small boat with reflector	4.0	3.7	6.8	0.5
7	Buoy with reflector	3.5	3.6	6.7	1.0
8	Buoy	3.5	3.0	5.6	0.5
9	Small 10 m long boat	2.0	3.0	5.6	1.4
10	Channel marker	1.0	1.0	1.9	0.1

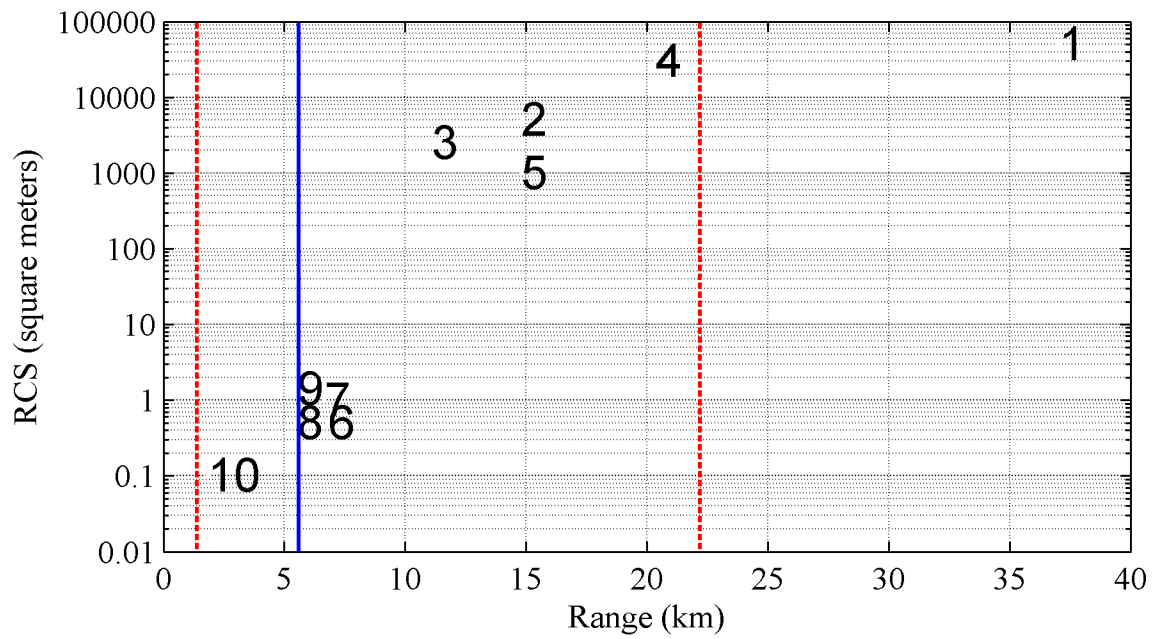


Figure 10. RCS and range for 10 IEC 62388 standard clutter free test cases with pulse range limits. Short and long pulses are separated by solid blue line at 5.6 km. Medium pulse ranges are between dashed red lines at 1.4 and 22.2 km.

4 MATHEMATICAL FOUNDATION

This section provides the mathematical description of our method to determine distance separation between the base stations and radar positions and frequency separation between the base stations and radar center frequencies required to mitigate unwanted out-of-band and spurious emissions so that IPC are met.

4.1 Powers, Power Ratios, and IPC

Signal, noise, and interference powers are referenced to the receiver input. The signal power is

$$s = \frac{1}{T} \int_{-T/2}^{T/2} s^2(t) dt \quad (6)$$

where T is the pulse period.

The receiver noise power is

$$n = \mathcal{E} \left\{ \left(\int_{-\infty}^{\infty} n(\tau) h_{if}(t - \tau) d\tau \right)^2 \right\} \quad (7)$$

where $\mathcal{E}\{\cdot\}$ is the expectation operator. When the noise power spectral density is constant,

$$n = kT_0 f_{rx} b_{if} \quad (8)$$

where k is Boltzman's constant, T_0 is the ambient temperature in degrees K, f_{rx} is the receiver noise factor, and b_{if} is the IF filter equivalent noise bandwidth.

The interference power is

$$i = \mathcal{E} \left\{ \left(\int_{-\infty}^{\infty} i(\tau) h_{if}(t - \tau) d\tau \right)^2 \right\} \quad (9)$$

The relationships between SNR, INR, and SINR power ratios are derived as follows:

$$\frac{s}{i+n} = \frac{s/n}{i/n+1} \quad (10)$$

$$i/n = \frac{s/n}{s/(i+n)} - 1 \quad (11)$$

For notational convenience we let $w = \frac{s}{n}$ represent SNR, $u = \frac{i}{n}$ represent INR, and $v = \frac{s}{i+n}$ represent SINR. W , U , and V are w , u , v respectively in dB. The w can be thought of as wanted

signal power normalized by the noise power and u as unwanted interfering signal power normalized by the noise power. Hence, (11) can be rewritten as

$$u = \frac{w}{v} - 1 \quad (12)$$

or

$$v = \frac{w}{u + 1} \quad (13)$$

and IPC baseline SNR, w_b , allowable INR, u_a , and allowable SINR, v_a , are related by

$$u_a = \frac{w_b}{v_a} - 1 \quad (14)$$

or

$$v_a = \frac{w_b}{u_a + 1} \quad (15)$$

4.2 Distance Separation with Spurious Attenuation

4.2.1 Constant SNR

Distance separation analysis for constant SNR is dependent on expressions for the received aggregate spurious emissions power and radar link reliability. SNR is assumed to be set to the baseline level, w_b . The expression for aggregate spurious emission power is a combination of the interference link budget in the previous background report [15] and the definition of spurious attenuation discussed in Appendix A

$$i(d_1, l_{spur}) = \sum_{n=1}^N i_{single}(d_n) = \sum_{n=1}^N \frac{\hat{p}_{ta} \hat{g}_t g}{\sqrt{l_d l_{bm} l_{pol} l_{cr}}} \cdot \frac{1}{\tilde{l}_{p,n}(d_n)} \cdot \frac{b_{if}}{l_{spur} b_{ref}} \quad (16)$$

where d_1 is the distance to the closest base station of the aggregate, d_n is the distance from the radar to the n -th base station, N is the number of base stations in the aggregate, \hat{p}_{ta} is the signal power in at the transmit antenna input, \hat{g}_t is the gain of the base station antenna in the direction of the radar, g is the gain of the radar antenna in the direction of the base station, l_d is the radome loss, l_{bm} is the integration beam shape loss, l_{pol} is the polarization loss between the base station and radar antennas, l_{cr} is the radar receiver circuit loss, \tilde{l}_p is the path loss from the base station to the radar, l_{spur} is the spurious attenuation, b_{ref} is the equivalent noise bandwidth of the reference filter, and b_{if} is the equivalent noise bandwidth of the radar IF filter.

The expression for reliability is

$$Pr\{\mathcal{U}(d_1, l_{spur}) < U_a\} = \int_{-\infty}^{U_a} f(U(d_1, l_{spur}))dU \quad (17)$$

i.e., the probability that INR is less than the allowable INR. The right side of this equation is the aggregate interference distribution function derived by Monte Carlo analysis in the previous background report.

4.2.2 Variable SNR

Distance separation analysis for variable SNR is dependent on expressions for the received aggregate spurious emissions power shown above, received radar signal power derived in the previous background report, and radar link reliability.

The received radar signal power is

$$s(d_{rt}) = \frac{p_{tx}g^2\sigma_{av}\lambda^2}{(4\pi)^3d_{rt}^4a^2(d_{rt})l_d l_{bm}l_{ct}l_{cr}m} \quad (18)$$

where p_{tx} is the radar source power, g is the radar antenna gain, σ_{av} is the target mean RCS, λ is the wavelength, d_{rt} is the radar to target range, $a(d_{rt})$ is the radar to target excess path loss which varies with distance, l_d is the radome loss, l_{bm} is the integration beam shape loss, l_{ct} is the radar transmitter circuit loss, l_{cr} is the radar receiver circuit loss, and m is the excess power margin.

The expression for radar link reliability is

$$Pr\{\mathcal{W}(d_{rt}) \geq W_b, \mathcal{V}(d_1, l_{spur}) \geq V_a\} \quad (19)$$

i.e., the joint probability that the SNR is greater than or equal to the base line SNR and the SINR is greater than or equal to the allowable SINR. An expression for the practical computation of this probability is derived as follows. For notational convenience, the independent variables d_{rt} , d_1 , and l_{spur} are not explicitly stated.

The joint probability can be written in integral form as

$$Pr\{\omega \geq w_b, \nu \geq v_a\} = \int_{w_b}^{\infty} \int_{v_a}^{\infty} f(w, \nu)dvdw \quad (20)$$

But $f(w, \nu) = f(\nu|w)f(w)$ and the upper limit of the inner integral is w when interference is not present, i.e. $u = 0$, so

$$Pr\{\omega \geq w_b, \nu \geq v_a\} = \int_{w_b}^{\infty} \left[\int_{v_a}^w f(\nu|w)dv \right] f(w)dw \quad (21)$$

We now want to express the inner integral in terms of u . Since

$$f(v|w)dv = f(u|w)du \quad (22)$$

and u is independent of w we have

$$\int_{v_a}^w f(v|w)dv = \int_0^{\frac{w}{v_a}-1} f(u)du \quad (23)$$

In other words the complementary cumulative distribution function of v is equal to the cumulative distribution function of u

$$Pr\{v > v_a|w\} = Pr\left\{u < \frac{w}{v_a} - 1\right\} \quad (24)$$

Finally

$$Pr\{w \geq w_b, v \geq v_a\} = \int_{w_b}^{\infty} \left[\int_0^{\frac{w}{v_a}-1} f(u)du \right] f(w)dw \quad (25)$$

In addition we can write this in terms of decibels since

$$f(u)du = f(U)dU \quad (26)$$

and

$$f(w)dw = f(W)dW \quad (27)$$

Consequently, reliability is also

$$Pr\{W \geq W_b, V \geq V_a\} = \int_{W_b}^{\infty} \left[\int_{-\infty}^{10 \log_{10} \left(\frac{10^{0.1W}}{10^{0.1V_a}} - 1 \right)} f(U)dU \right] f(W)dW \quad (28)$$

Inner and outer integrals are computed with segmented log normal distribution functions. The method for computing the outer integral is documented in the description of the ITM in the previous background report. A fast method for computing the inner integral is provided in Appendix B.

4.3 Distance Separation with FDR

The expression for aggregate unwanted emission power is a combination of the interference link budget in the previous background report and the definition of frequency dependent rejection discussed in Appendix A

$$i(d_1, \Delta f) = \sum_{n=1}^N i_{single}(d_n) = \sum_{n=1}^N \frac{\hat{p}_{ta} \hat{g}_t g}{\sqrt{l_d l_{bm} l_{pol} l_{cr}}} \cdot \frac{1}{\tilde{l}_{p,n}(d_n)} \cdot \frac{1}{l_{fdr}(\Delta f)} \quad (29)$$

This is the same expression as that used for spurious emissions with the substitution

$$l_{fdr}(\Delta f) = \frac{l_{spur} b_{ref}}{b_{if}} \quad (30)$$

Consequently we can convert spurious attenuation distance separation results to frequency separation results by finding the Δf which satisfies (30).

5 RESULTS

5.1 Parameters

Parameters for these scenarios are explained in detail in the previous background report [15]. Table 2 summarizes relevant radar and BRS parameters.

Table 2. Radar and BRS parameters used for analysis.

Parameter	Value	Note
\hat{p}_{ta}	13.0 dBW	20 W for 10 MHz bandwidth signal at antenna
\hat{g}_t	15.0 dB	
l_d	1.0 dB	Transmission and reception
l_{bm}	1.6 dB	Transmission and reception
l_{sp}	1.8 dB	
l_{cr}	2.7 dB	
l_{ct}	2.7 dB	
l_s	9.8 dB	
l_{pol}	3.0 dB	Radar is horizontally polarized. BRS is slant polarized.
p_{tx}	44.8 dBW	30 kW at source
g	27.0 dB	
f_{rx}	5.0 dB	Referred to limiter input

5.2 Interference Protection Criteria

IPC were determined for the IEC 62388 long and short pulses at a 40 rpm antenna rotation rate. As shown in Table 3, the long and short pulses were integrated 6 and 14 times, respectively.

Table 3. Baseline ideal SNR for a 1.9 degree beam-width antenna at baseline performance $0.8 P_d$ and $10^{-4} P_{fa}$. PW is pulse width, PRF is pulse repetition frequency, BW is IF filter bandwidth, RR is rotation rate, and n_p is the number of pulses integrated.

Pulse	PW (ns)	PRF (Hz)	BW (MHz)	RR (rpm)	n_p	Ideal SNR (dB)	
						Swerling 0	Swerling 1
Short	50	1800	20	40	14	2.31	7.58
Long	800	785	3	40	6	4.83	10.03

The INR are determined from the GN interference radar performance curves in Figures 11 and 12. Conditions used to create the curves include Swerling 1 RCS fluctuation, baseline performance of $\mathcal{P}_d = 0.8$ and $\mathcal{P}_{fa} = 10^{-4}$, and non-coherent integration. The equations used to create the plot are

$$u = \frac{w_b(n_p, \mathcal{P}_{d,b}, \mathcal{P}_{fa})}{v(n_p, \mathcal{P}_{d,a}, \mathcal{P}_{fa})} - 1 \quad (31)$$

based on (12) and,

$$\text{degraded performance percentage} = \left(\frac{\mathcal{P}_{d,b} - \mathcal{P}_d}{\mathcal{P}_{d,b}} \right) \cdot 100\% \quad (32)$$

where $\mathcal{P}_{d,b}$ is the baseline performance probability of detection, $\mathcal{P}_{d,a}$ is the allowable probability of detection, n_p is the number of pulses integrated, and w_b is the baseline performance SNR.

The curves show INRs of -6, -9, and -12 dB have approximately 5.5%, 2.8%, and 1.4% degradation, respectively. Differences between long and short pulses are negligible. These INRs raised the radar receiver noise floor of approximately 1.0, 0.5, and 0.25 dB, respectively, as shown in Appendix C. Baseline and degraded conditions for the long and short pulse widths are shown in Table 4.

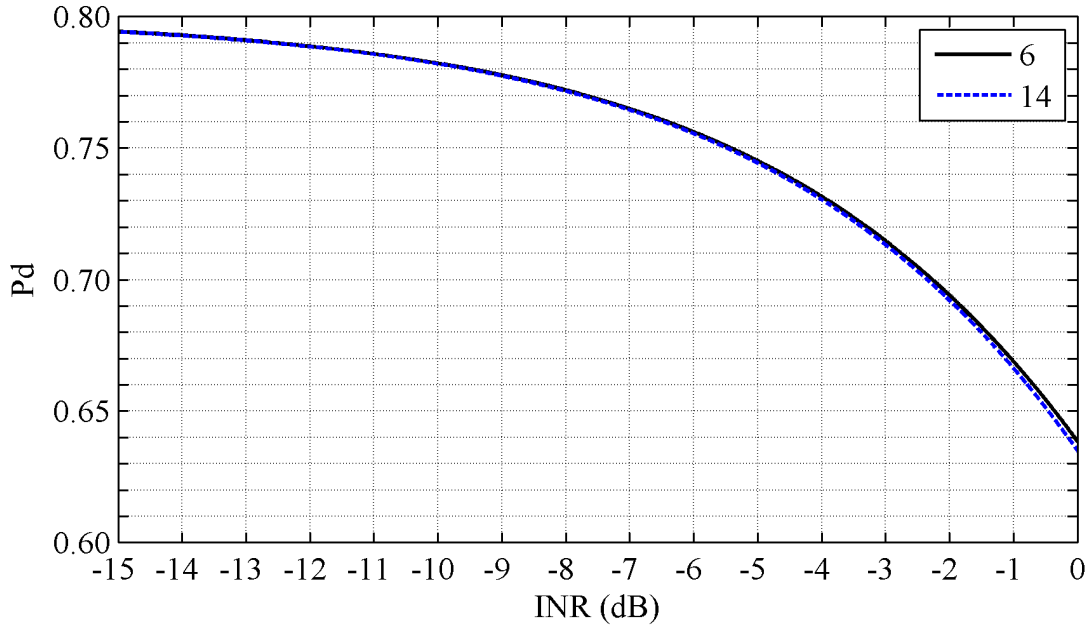


Figure 11. Radar performance with GN interfering signal, Swerling 1 target, non-coherent integration performance, and baseline performance of $0.8 P_d$, $10^{-4} P_{fa}$. The long and short pulses were integrated 6 and 14 times, respectively.

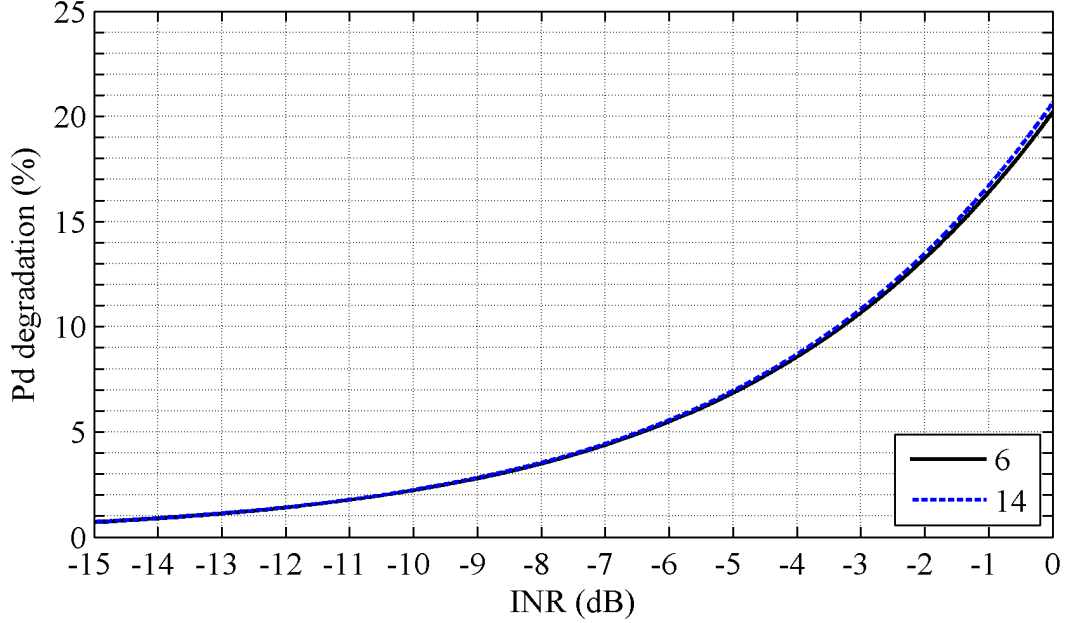


Figure 12. Radar performance degradation with GN interfering signal, Swerling 1 target, non-coherent integration, and baseline performance of $0.8 P_d$, $10^{-4} P_{fa}$. The long and short pulses were integrated 6 and 14 times, respectively.

Table 4. Relevant IPC parameters for baseline $0.8 P_d$, $10^{-4} P_{fa}$ with long and short pulse widths. S, I, and N are evaluated at the receiver input.

Pulse width	Baseline SNR (dB)	Allowable INR (dB)	Allowable degradation (P_d /%)	Allowable SINR (dB)	S (dB)	I (dB)	N (dB)
Long	11.83	-6	0.76/5.5	10.87	-92.40	-110.23	-104.23
Long	11.83	-9	0.78/2.8	11.32	-92.40	-113.23	-104.23
Long	11.83	-12	0.79/1.4	11.57	-92.40	-116.23	-104.23
Short	9.38	-6	0.76/5.6	8.41	-86.61	-101.99	-95.99
Short	9.38	-9	0.78/2.8	8.87	-86.61	-104.99	-95.99
Short	9.38	-12	0.79/1.4	9.12	-86.61	-107.99	-95.99

5.3 Interference Power Distributions

The aggregate interference power distribution is determined by Monte Carlo analysis using the ITM propagation model as shown in the previous background report. Figure 13 shows the results of this analysis for distances to the closest base station, d_1 , at 1 km and then at 5 km steps starting at 5 km. These results are for 60 dB of spurious attenuation. The most distinctive feature of these curves is how variability increases with distance. The INR for the 1 and 5 km curves is relatively constant.

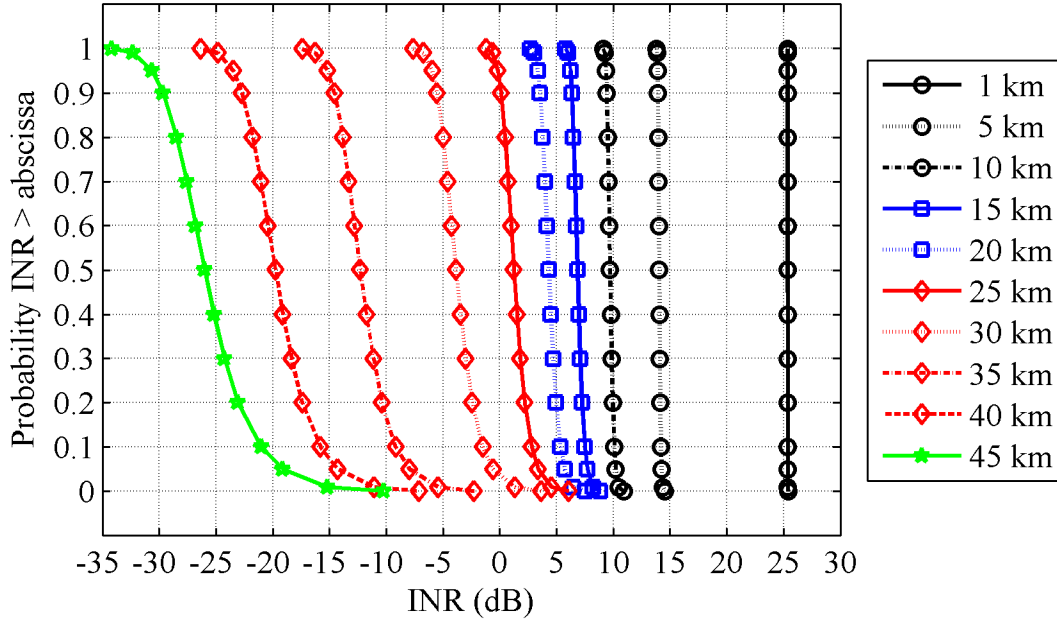


Figure 13. INR distributions at various distances to the closest base station when there is 60 dB spurious attenuation.

5.4 Distance separation with spurious attenuation

5.4.1 Constant SNR

Results were calculated for single 10 MHz bandwidth signal with spurious attenuations ranging from 56 dB to as much as 100 dB, where 56 dB is the ITU minimum amount of spurious attenuation for the U.S. These results are valid for both long and short pulses. Methods for converting between spurious attenuation, L_{spur} , transmitted power density in the reference bandwidth, Ψ_{ref} , and effective isotropic radiated power in the reference bandwidth, Z_{ref} , are provided in Appendix D.

The separation distances between the base station and the radar at various reliabilities and spurious attenuations for a -6 dB INR are presented in Table 5 and shown in Figure 14. Results for -9 and -12 dB INR are provided in Appendix H. In the tables, separation distances < 1 km occur when the allowable INR was not reached at the 1 km ITM distance limit because of high spurious attenuation. Greater spurious attenuation resolution, perhaps 1 dB instead of the current 5dB, is needed to determine a better estimate of spurious attenuation needed at 1 km.

The results show that greater separation distances are needed for higher reliabilities and lower spurious attenuations when all other parameters are held constant. Close separation distances with little or no change in reliability can be achieved with increased spurious attenuation.

Results for 90% reliability are provided for all INR in Table 6. The results show that more than 90 dB spurious attenuation is required to achieve 90% reliability at a 1 km separation distance at -6 and -9 dB INR. More than 95 dB spurious attenuation is needed at -12 dB INR.

The ETSI spurious emission requirement outside the BRS operating band is -52 dBm/MHz. This limit corresponds to 95 dB spurious attenuation when 20 W of power is at the transmit antenna input, which is adequate for -6 and -9 dB INR but not for -12 dB.

Table 5. Analysis results for -6.0 dB allowable INR.

Parameter			Separation distance, d_{min} (km)						
L_{spur}	Ψ_{ref}	Z_{ref}	Reliability						
dB	dBm/MHz	dBm/MHz	50%	60%	70%	80%	90%	95%	99%
56	-13	2	33.6	33.9	34.2	34.7	35.5	36.4	38.8
60	-17	-2	31.2	31.5	31.8	32.1	32.8	33.6	35.4
65	-22	-7	27.7	28.10	28.6	29.1	29.6	30.2	31.6
70	-27	-12	20.4	20.7	21.1	21.7	22.9	23.7	26.4
75	-32	-17	11.1	11.2	11.4	11.6	11.9	12.2	13.0
80	-37	-22	5.0	5.0	5.0	5.1	5.1	5.2	5.3
85	-42	-27	2.3	2.3	2.3	2.3	2.3	2.3	2.3
90	-47	-32	1.1	1.2	1.2	1.2	1.2	1.2	1.2
95	-52	-37	< 1	< 1	< 1	< 1	< 1	< 1	< 1

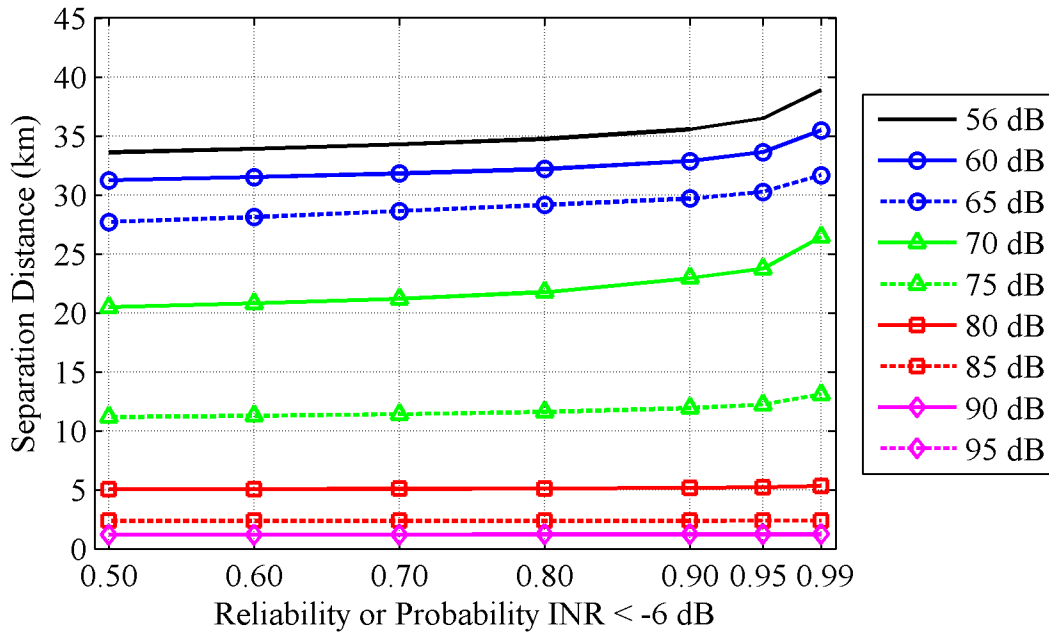


Figure 14. Separation distance versus reliability for -6 dB INR. 95 dB attenuation produces separation distances less than the 1 km propagation model limit and is not shown.

Table 6. Separation distances for all INR at 90% reliability.

Parameter			Separation distance, d_{min} (km)		
L_{spur}	Ψ_{ref}	Z_{ref}	INR (dB)		
dB	dBm/MHz	dBm/MHz	-6	-9	-12
56	-13	2	35.5	37.7	40.1
60	-17	-2	32.8	34.8	37.0
65	-22	-7	29.6	31.5	33.5
70	-27	-12	22.9	27.6	30.3
75	-32	-17	11.9	18.3	24.6
80	-37	-22	5.1	8.5	14.0
85	-42	-27	2.3	3.7	6.0
90	-47	-32	1.2	1.7	2.7
95	-52	-37	< 1	< 1	1.3
100	-57	-42	< 1	< 1	< 1

5.4.2 Variable SNR

Variable SNR analysis requires knowledge of radar target height, range, and RCS characteristics. We used the targets of the ten IEC 62388 standard clutter free test cases because of their importance to maritime radar designers. The SNR distributions for the test cases are shown in Figure 15. Cases 1–9 and case 10 were analyzed with the long and short pulses, respectively. The 99% excess power margin, used to compensate for variations in RCS because of target aspect, materials, and shape, has been removed by reducing the RCS as discussed in the previous background report. With the excess power margin removed the 99% SNR quantile is equal to the baseline SNR.

Figure 16 shows the INR for the 10 test cases at these separation distances with spurious attenuation set to 60 dB. The separation distance between the radar and the closest base station is set to the radar to target range plus a 1 km base station to target distance.

Table 7 summarizes final results. The least spurious attenuation, 56 dB, was required by the furthest target, Case 1. The most spurious attenuation, 85.1 dB, was required by the closest target, Case 10. Appendix E shows examples of the raw data from which these results are drawn.

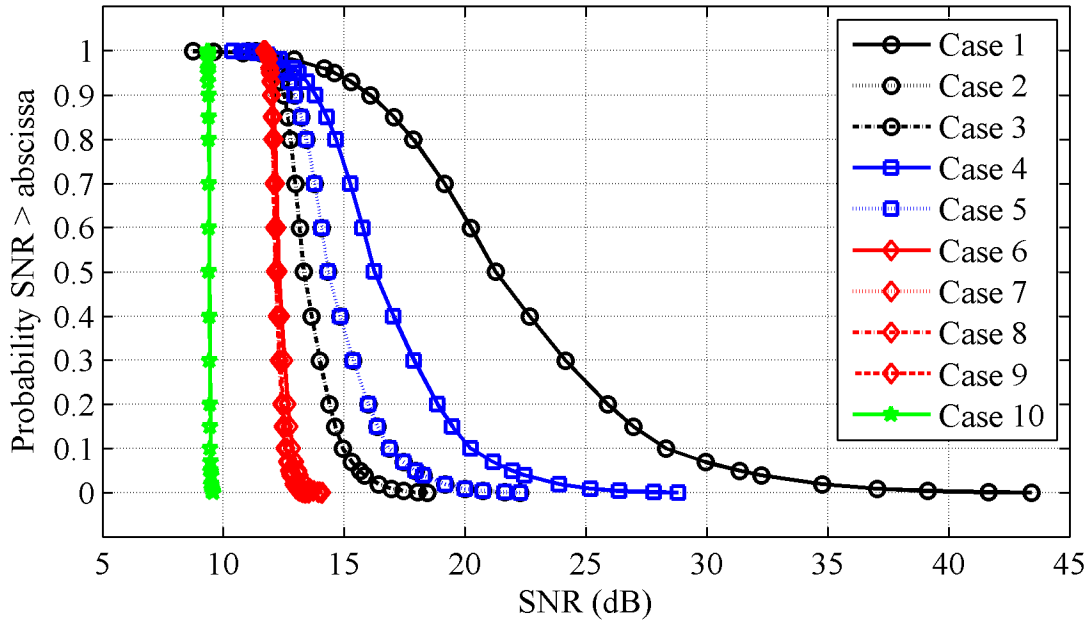


Figure 15. SNR distributions for 10 IEC 62388 standard clutter free test cases with power margin removed. Only seven curves are visible because cases 2 and 5, 6 and 7, and 8 and 9 have similar target parameters.

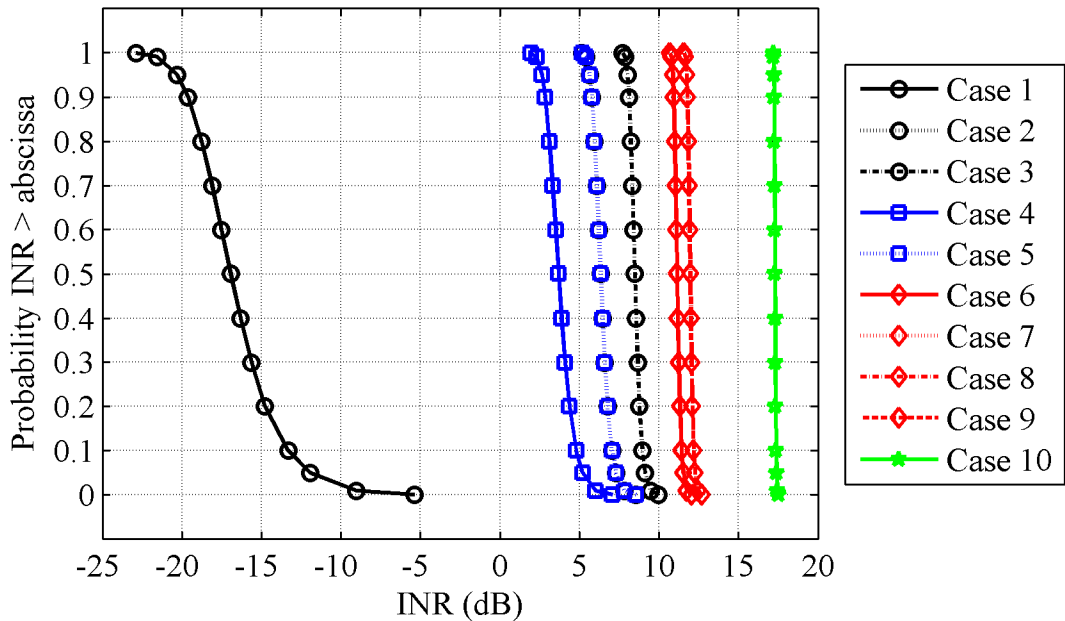


Figure 16. INR distributions for 10 IEC 62388 clutter free test cases with spurious attenuation set to 60 dB. The separation distance between the radar and the closest base station is set to the radar to target range plus a 1 km base station to target distance. Only seven curves are visible because cases 2 and 5, 6 and 7, and 8 and 9 have similar target distances.

Table 7. Spurious attenuation for IEC 62388 standard clutter free test cases for 90% reliability.

Case	Description	Height (m)	Range		RCS (m ²)	<i>L_{spur}</i> (dB)		
			nmi	km		-6 dB INR	-9 dB INR	-12 dB INR
1	60 m high shoreline	50.0	20.0	37.0	50000.0	<56	<56	<56
2	6 m high shoreline	5.0	8.0	14.8	5000.0	68.6	69.9	70.9
3	3 m high shoreline	2.5	6.0	11.1	2500.0	72.2	73.7	74.7
4	SOLAS ship > 5000gt	10.0	11.0	20.4	30000.0	63.6	64.7	65.3
5	SOLAS ship > 500gt	5.0	8.0	14.8	1000.0	68.6	69.9	70.9
6	Small boat with reflector	4.0	3.7	6.8	0.5	77.9	70.6	83.6
7	Buoy with reflector	3.5	3.6	6.7	1.0	77.1	79.2	81.1
8	Buoy	3.5	3.0	5.6	0.5	78.4	80.4	83.1
9	Small 10 m long boat	2.0	3.0	5.6	1.4	78.3	80.3	82.9
10	Channel marker	1.0	1.0	1.9	0.1	85.1	87.5	90.1

5.4.3 Comparison of constant SNR to variable SNR results

Here we compare spurious attenuation levels obtained using variable SNR against those obtained using constant SNR. The constant SNR results have a short radar to target range regardless of the separation distance.

Results of the comparison for -6 dB INR, 90% reliability are shown in Figure 17. Corresponding comparisons for -9 and -12 dB INR are provided in Appendix H. Variable SNR cases can be identified by their separation distances which are 1 km more than the radar to target distance. Case 1 is not shown because the required spurious attenuation is below the minimum tested. Cases 8 and 9 at 6.6 km and Cases 2 and 5 at 15.8 km are indistinguishable because they have nearly identical spurious attenuation requirements due to similarities in target height and range.

The methods disagree the most at longer radar to target ranges. As an example, Case 4 at 21.4 km required 7 dB less attenuation with variable SNR than constant SNR. This difference increased even more with decreasing INR, as shown in Table 8. From this we can conclude that the constant SNR method, where radar to target range is short regardless of separation distance, provides an upper bound on the amount of spurious attenuation needed.

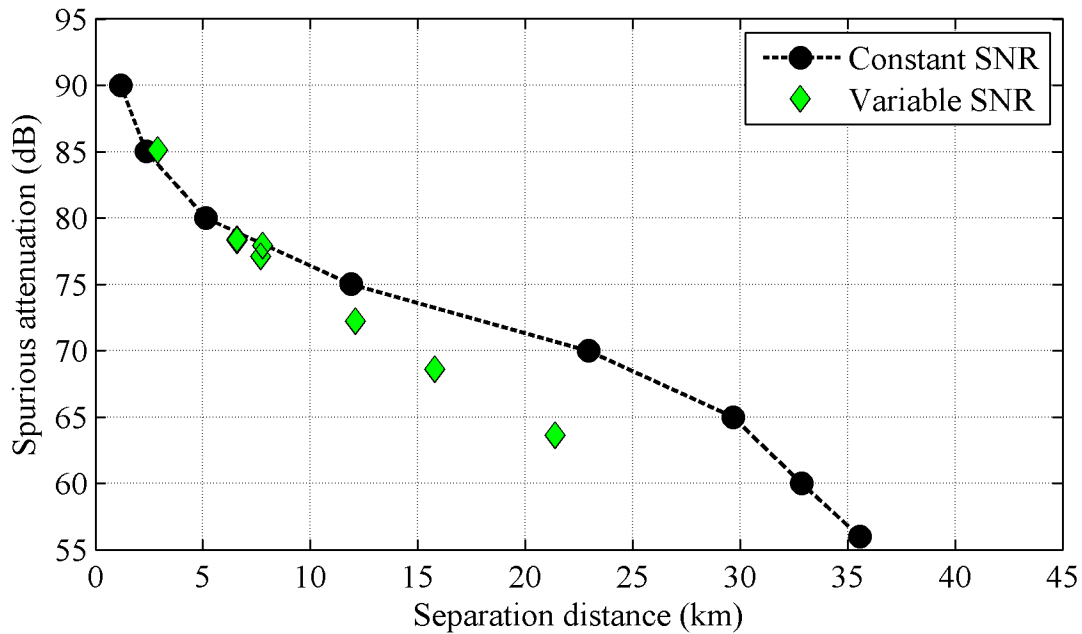


Figure 17. Comparison of constant and variable SNR results for -6 dB INR and 90% reliability.

Table 8. Spurious attenuation for IEC 62388 standard clutter free test cases using constant SNR (C) and variable SNR (V) for 90% reliability. Case 1 difference is not available (NA) because the required spurious attenuation is below the minimum tested.

Case	Description	Range (km)	-6 dB INR			-9 dB INR			-12 dB INR		
			L_{spur} (dB)		Diff (dB)	L_{spur} (dB)		Diff (dB)	L_{spur} (dB)		Diff (dB)
			V	C		V	C		V	C	
1	60 m high shoreline	37.0	NA	NA	NA	NA	NA	NA	NA	NA	NA
2	6 m high shoreline	14.8	68.6	73.2	-4.6	69.9	76.3	-6.4	70.9	79.2	-8.3
3	3 m high shoreline	11.1	72.2	74.9	-2.7	73.7	78.1	-4.5	74.7	81.2	-6.5
4	SOLAS ship > 5000gt	20.4	63.6	70.7	-7.1	64.7	73.4	-8.7	65.3	76.5	-11.2
5	SOLAS ship > 500gt	14.8	68.6	73.2	-4.6	69.9	76.3	-6.4	70.9	79.2	-8.3
6	Small boat with reflector	6.8	77.9	78.0	-0.1	80.6	80.8	-0.2	83.6	83.9	-0.3
7	Buoy with reflector	6.7	77.1	78.1	-1.0	79.2	80.9	-1.7	81.1	84.0	-2.9
8	Buoy	5.6	78.4	78.9	-0.5	80.4	82.0	-1.6	83.1	84.7	-1.6
9	Small 10 m long boat	5.6	78.3	78.9	-0.6	80.3	82.0	-1.7	82.9	84.7	-1.8
10	Channel marker	1.9	85.1	84.0	1.1	87.5	87.1	0.4	90.1	89.7	0.4

5.5 Distance and frequency separation with FDR

FDR is calculated from the transmitted PSD and receiver IF filter frequency response. In this report we use measured, filtered, and spectrum emission mask (SEM) PSDs. The measured PSD was discussed in the previous background report. The filtered PSD, described in Appendix F is designed to reduce unwanted emissions in the 2700–2900 MHz radar band. The SEM PSD is described in Appendix D.2. Justification for using an ideal short pulse, 20 MHz bandwidth, IF filter frequency response which falls off at 80 dB/decade outside the 3 dB bandwidth is provided in Appendix G.

Figure 18 shows the measured, filtered, and SEM PSDs used for calculating FDR. The measured and filtered PSD powers are adjusted with the assumption of a 26 dBm/100 kHz or 46 dBm/10 MHz signal power. The SEM is adjusted to a 100 kHz bandwidth.

Figure 19 shows the results of the FDR calculations. Because frequency separation is defined as the difference between the transmitted and received center frequencies, the positive separation frequencies are due to radar center frequencies below the 2683.5 MHz BRS center frequency and the negative separation frequencies are due to radar center frequencies above the 2683.5 MHz BRS center frequency. Our interest is in the negative separation frequencies, where the filtered PSD has the most FDR, followed by the SEM and the measured PSD.

Frequency separation needed to satisfy allowable INR is determined from the constant SNR spurious attenuation requirements in Table 6, which we have already established as worst case. First, the spurious attenuation is converted to FDR using (30). Then, frequency separation is determined from the FDR. As an example, converting the -6 dB INR, 90% reliability, greater than 90 dB spurious attenuation requirement at 1 km separation distance from Table 6 yields a greater than 77 dB FDR requirement. Figure 19 shows that this FDR corresponds to 92.8 MHz for the filtered PSD and 99.7 MHz for the SEM.

Frequency separation results for all INR are summarized in Table 9. Those that never obtain the FDR required to meet IPC are labeled NA. The SEM requires slightly more frequency separation than the filtered PSD at -6 and -9 dB INR. SEM and filtered PSD results do not change between -6 and -9 dB INR. The filtered PSD is the only one that meets the IPC at -12 dB INR, where it shows a slight increase compared to -9 dB INR.

The combined separation distance and frequency separation needed for the allowable IPC can also be determined. We do this by converting separation distance versus reliability curves for various spurious attenuations to various FDR. We can then plot any combination of separation distance and frequency separation that meets a specified reliability. Results of this analysis using the -6 dB INR case in Figure 14 are shown in Figure 20. The results show that frequency separation can be reduced from 92.8 MHz to 54.6 MHz when the separation distance is increased from 1.2 km to 32.8 km.

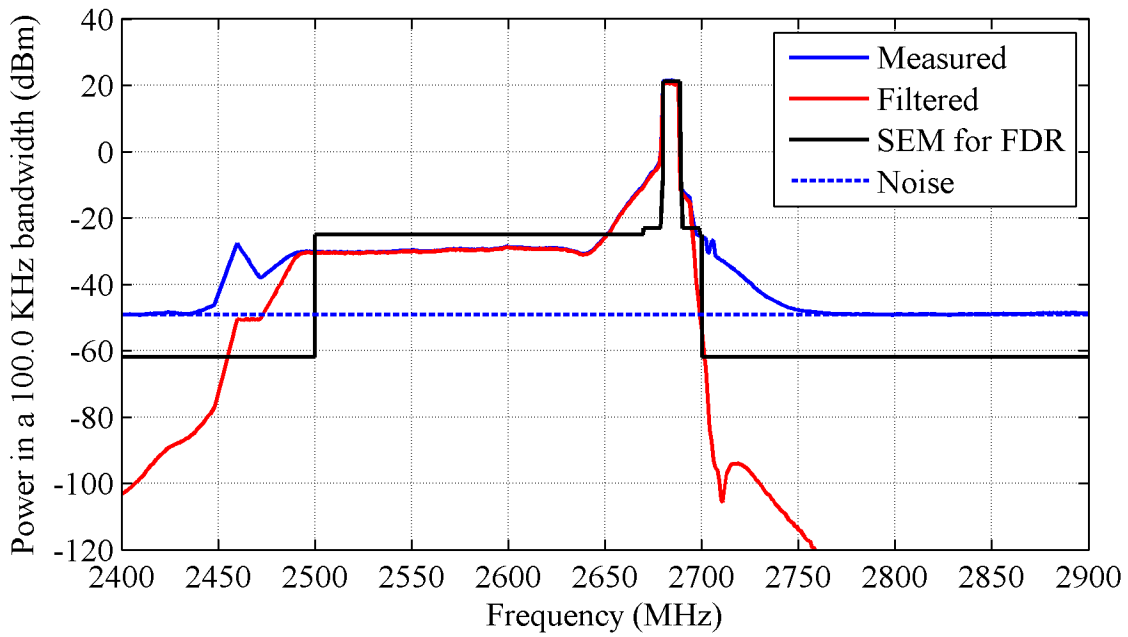


Figure 18. Measured PSD, filtered measured PSD, and SEM.

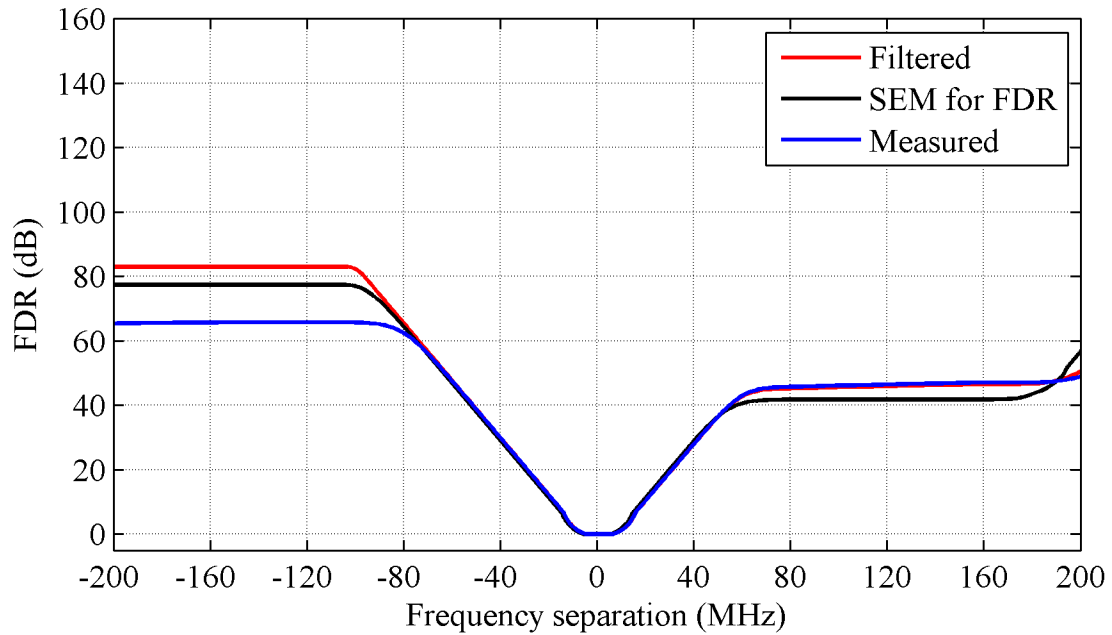


Figure 19. FDR for ideal short pulse, 20 MHz bandwidth, IF filter.

Table 9. Spurious attenuation, L_{spur} , FDR, L_{fdr} , and frequency separation, Δf , needed for 90% reliability for 20 MHz bandwidth short pulse at 1 km distance separation.

INR (dB)	L_{spur} (dB)	L_{fdr} (dB)	Δf (MHz)		
			Unfiltered	Filtered	SEM
-6	>90	>77	NA	>92.8	99.7
-9	>90	>77	NA	>92.8	99.7
-12	>95	>82	NA	>99.3	NA

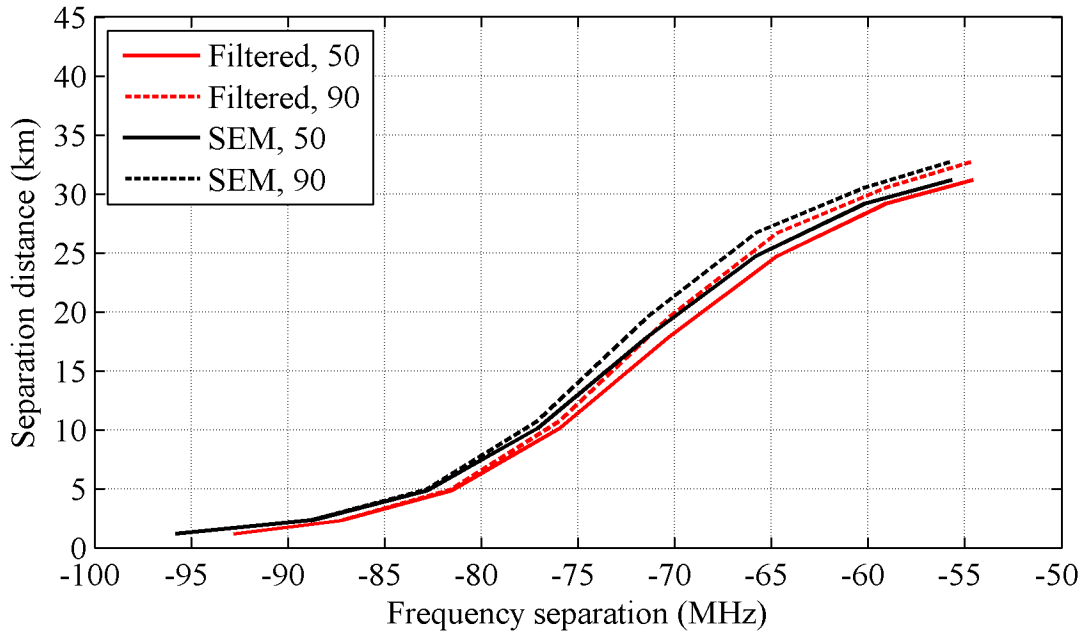


Figure 20. Separation distance versus frequency separation for 50 and 90% reliability with short pulse 20 MHz radar detection IF bandwidth when INR is -6 dB.

6 CONCLUSION

This report analyzes the effect of unwanted emissions from a broadband radio service (BRS) base station on magnetron radar receiver performance. This report builds upon the interference model developed in the previous background report [15] where we demonstrated that unwanted emissions were Gaussian distributed and aggregated. Results include distance separation and frequency separation that meet interference protection criteria (IPC). Baseline radar system performance was set at a 0.8 probability of detection and 10^{-4} probability of false alarm. Interference to noise ratios (INR) of -6, -9, and -12 dB were investigated.

Distance separation was computed from expressions for radar link reliability. Reliability in this context is dependent solely on radio wave propagation path loss variability. So that anomalous radio wave propagation ducting conditions do not influence results, 90% reliability is used. Two expressions for reliability were provided. One expression assumed constant radar signal to noise ratio (SNR) corresponding to short radar to target ranges. This method does not require knowing the radar to target link budget.

The other expression assumed variable SNR which is valid over any radar to target range. This method requires complete knowledge of the radar to target link budget. We used targets from the IEC 62388 standard clutter free test cases to set radar to target link budget parameters. Base station to radar path length was set to the radar to target range plus 1 km.

The constant SNR case is important because it can be easily applied to the most demanding case where the ship with the radar is close to the target and the base station. The expression for variable SNR is the most general and useful for situations where close radar to base station distances are not likely.

Distance separation calculations for constant SNR showed that 90 dB spurious attenuation could provide 90% reliability at a separation distance of 1.2 km when INR is -6 dB. The separation distance decreased below 1 km with 95 dB spurious attenuation. For reference, the ETSI -52 dBm/MHz unwanted emissions limit outside the BRS operating band corresponds to 95 dB spurious attenuation.

Results for variable SNR agreed with those using constant SNR at short radar to target range. However, as radar to target range increased, less spurious attenuation was needed. The largest difference was with case 4, a SOLAS ship 21.4 km away from the radar, where 7.1 dB less spurious attenuation was needed when INR is -6 dB. Consequently the constant SNR reliability expression can be considered worst case.

We also showed how frequency separation could be computed by replacing spurious attenuation by an expression for FDR. The FDR were calculated from measured PSD, filtered PSD, spectrum emission mask, and idealized IF filter frequency responses that corresponded with measured filter frequency responses. SNR was assumed to be constant so results are worst case. The results showed that 90 % reliability IPC could be met at 1.2 km separation distance with 92.8 MHz and 99.7 MHz for the filtered PSD and SEM when INR is -6 dB. We found that filtered PSD frequency separation can be reduced from 92.8 MHz to 54.6 MHz when the distance separation is increased to 32.8 km.

Results for the -9 dB and -12 dB INR cases differed in most cases. For example, the separation distance for the constant SNR case increased to 1.7 and 2.7 km with 90 dB spurious attenuation for INR of -9 and -12 dB, respectively. For variable SNR, case 4 required 8.7 and 11.2 dB less spurious attenuation than constant SNR for INR of -9 and -12 dB, respectively. Frequency separation did not increase when the INR was decreased to -9. However it did increase to 99.3 MHz when INR was decreased to -12 dB.

The results in this report are encumbered with two caveats. First, the results are for a frequency division duplexing (FDD) BRS base station signal that occupies one 10 MHz BRS channel. Results need to be adjusted to accommodate more channels. Second, these results are based on magnetron radar signal processing. Additional analysis is needed to assess the impact to solid-state radar receivers because their signal processing is very different from that in the magnetron radar receiver. The signal processing affects receiver sensitivity and IF selectivity and estimates of separation distance and frequency separation need to take this into account.

7 ACKNOWLEDGEMENTS

This work was sponsored by the U.S. Coast Guard Spectrum Management Telecommunications Policy Division, U.S. Coast Guard CG-652, 2100 2nd St. SW Stop 7101, Washington DC 20593-7101. The authors would like to acknowledge Fred Mistichelli (former Division Chief), Joseph Hersey (former Division Chief), and Daniel Freedman (former Spectrum Engineer) for their sponsorship.

The authors would also like to acknowledge David Turnage, Research and Development Manager, Kelvin Hughes Ltd.; Lawrence Cohen, Electronics Engineer, U.S. Naval Research Laboratory; Jon Higham, Program Coordinator, United Kingdom Office of Communication (OFCOM); David G. Money, consultant to the OFCOM; and Richard Rees, Spectrum Policy and Technical Standards Manager, United Kingdom Maritime and Coastal Agency for sharing their insights into this issue.

Finally, the authors would also like to acknowledge Al Romero, Visual Information Specialist, of the National Oceanic and Atmospheric Administration (NOAA) for creating the illustrative figures.

8 REFERENCES

- [1] International Telecommunication Union, “Procedures for determining the potential for interference between radars operating in the radiodetermination service and systems in other services,” Recommendation ITU-R M.1461-1, July 2003.
- [2] International Telecommunication Union, “Tests illustrating the compatibility between maritime radionavigation radars and emissions from radiolocation radars in the band 2900–3100 MHz,” Report ITU-R M.2032, 2003.
- [3] F. Sanders et. al., “Effects of RF interference on radar receivers,” NTIA Report TR-06-444, September 2006, <http://www.its.bldrdoc.gov/publications/2481.aspx>.
- [4] J.E. Carroll, G.A. Sanders, F.H. Sanders, and R.L. Sole, “Case study: Investigation of interference into 5 GHz weather radars from unlicensed national information infrastructure devices, Part I,” NTIA Technical Report TR-11-473, November 2010, <http://www.its.bldrdoc.gov/publications/2548.aspx>.
- [5] A. Paul et. al., “Interference protection criteria,” NTIA Report 05-432, October 2005, <http://www.its.bldrdoc.gov/publications/2462.aspx>.
- [6] International Telecommunication Union, “Studies on frequency-related matters on International Mobile Telecommunications and other terrestrial mobile broadband applications”, Resolution 233 (WRC-12), The World Radiocommunication Conference (Geneva, 2012)
- [7] International Electrotechnical Commission, “Maritime navigation and radiocommunication equipment and systems – Shipborne radar – Performance requirements, methods of testing and required test results,” IEC 62388, Edition 1.0, 2007-12.
- [8] International Maritime Organization, “Adoption of the revised performance standards for radar equipment,” Annex 34, Resolution MSC.192(79), December 6, 2004.
- [9] Institute for Electrical and Electronic Engineer, “IEEE recommended practice for the analysis of in-band and adjacent band interference and coexistence between radio systems,” IEEE Std 1900.2-2008, July 29, 2008.
- [10] United Kingdom of Great Britain and Northern Ireland, “Radar adjacent band selectivity,” Recommendation ITU-R 5b/389-E, November 18, 2009.
- [11] U.S. Department of Commerce, National Telecommunications and Information Administration, “An assessment of the near-term viability of accommodating wireless broadband systems in the 1675–1710 MHz, 1755–1780 MHz, 3500–3650 MHz, and 4200–4220 MHz, 4380–4400 MHz bands,” October 2010, http://www.ntia.doc.gov/files/ntia/publications/fasttrackevaluation_11152010.pdf.
- [12] European Telecommunications Standards Institute, “Technical Specification, Digital cellular telecommunications system (Phase 2+); Universal Mobile Telecommunications

System (UMTS); LTE; E-UTRA, UTRA, and GSM/Edge; Multi-Standard Radio (MSR) Base Station (BS) radio transmission and reception,” ETSI TS 137 104 version 11.2.1 Release 11, October 2012.

- [13] International Telecommunication Union Joint Task Group 4-5-6-7, Appendix 1 “Characteristics of terrestrial IMT-Advanced systems for frequency sharing/interference analyses” in Attachment 1, “Protection criteria, system characteristics, related materials on modelling considerations and sharing studies already performed or underway in ITU-R related to the terrestrial services” in Annex 2 “Compilation of material maintained by the Joint Task Group 4-5-6-7 working groups” of Report on the Fourth meeting of the Joint Task Group 4-5-6-7, Document 4-5-6-7/393-E, October 30, 2013.
- [14] WiMAX Forum, “Mobile WiMAX – Part 1: A Technical Overview and Performance Evaluation,” WiMAX Forum white paper, August 2006.
- [15] R. Achatz, P. McKenna, R. Dalke, N. DeMinco, F. Sanders, and J. Carroll, “Effect of broadband radio service reallocation on 2900–3100 MHz band marine radars: Background,” NTIA Report TR-15-513, April 2015. <http://www.its.bltdrdoc.gov/publications/2795.aspx>
- [16] International Telecommunication Union, “Unwanted emissions in the spurious domain,” Recommendation ITU-R SM.329-10, February 2003.
- [17] A. Piotrowski, “In band interference to radar for Swerling targets,” in *Proc. of the 2008 IEEE International Conference on Radar*, September 2008, pp. 379–385.

APPENDIX A: UNWANTED SIGNAL POWER

A.1 Basic Frequency Dependent Interference Model

A basic frequency dependent interference model is shown in Figure A-1. The transmitter is on the left beginning with the transmitter source (TX) and ending with an antenna (TX ANT). The transmitter source and filter are separated by transmission loss. Unwanted emissions can be mitigated with the transmitter filter (TX filter). The receiver in another system begins with an antenna (RX ANT) and ends with a receiver filter (RX Filter). The receiver antenna and filter are separated by receiver loss. The transmitter and receiver antennas are assumed to be pointed directly at each other. The transmitter and receiver antennas are separated by path and polarization loss.

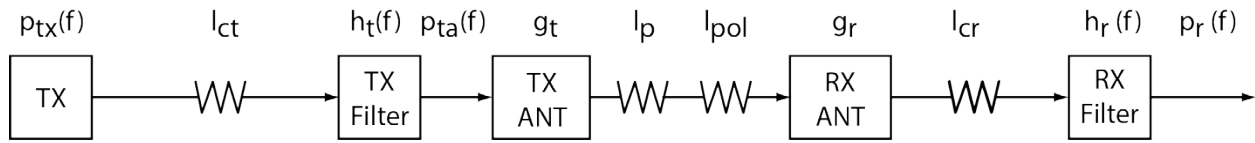


Figure A-1. Basic interference model. TX represents the transmitter source, TX Filter represents the transmitter filter, ANT represents the antenna, and RX filter represents the receiver filter.

The parameters in the Figure are defined as

- $p_{tx}(f)$ source power spectral density
- l_{ct} transmitter circuit loss
- $h_t(f)$ transmitter filter transfer function
- $p_{ta}(f)$ transmitted power spectral density
- g_t transmitter antenna gain
- $l_p(d)$ propagation path loss and d is path distance
- l_{pol} polarization loss
- g_r receiver antenna gain
- l_{cr} receiver circuit loss
- $h_r(f)$ receiver filter transfer function
- $p_r(f)$ received power spectral density

The frequency dependent parameters are expressed as low-pass complex-baseband signals centered at 0 Hz.

A.2 Transmitted Unwanted Signal Power

The ITU divides the transmitted signal power spectral density (PSD) into necessary bandwidth, out-of-band (OOB), and spurious domains [A-1] [A-2]. Power in the OOB and spurious domains are collectively referred to as unwanted. Figure A-2 shows a PSD with ITU domains.

The OOB domain lies between the necessary bandwidth and spurious domains. In general, the out-of-band domain extends from the edge of the necessary bandwidth to 250% of the necessary bandwidth from the center frequency. Mathematically the necessary bandwidth domain is

$$|\Delta f| < 0.5b_{nec} \tag{A-1}$$

the OOB domain is

$$0.5b_{nec} \leq |\Delta f| \leq 2.5b_{nec} \tag{A-2}$$

and the spurious domain is

$$|\Delta f| > 2.5b_{nec} \tag{A-3}$$

where the difference between the transmit frequency, f_t , and any other frequency is defined as $\Delta f = f_t - f$.

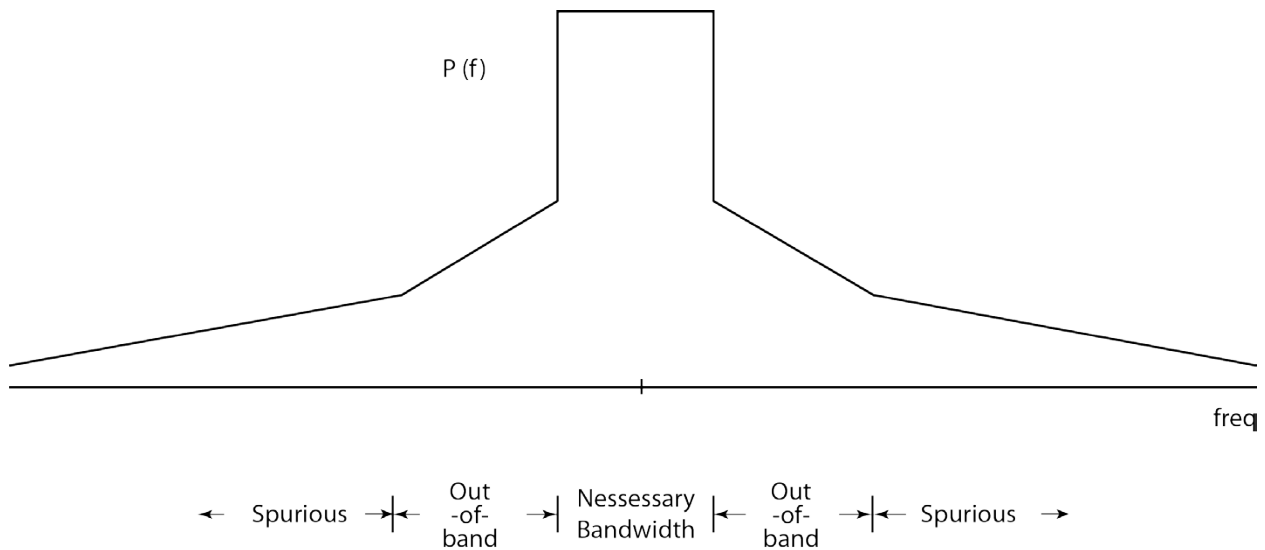


Figure A-2. Hypothetical PSD with ITU domains.

The necessary bandwidth domain contains most of the modulated signal power. Power in the spurious domain is due to effects incidental to transmission such as amplification, frequency conversion, and parasitic resonance. Power in the OOB domain is a mixture of modulated and incidental signals.

The ITU limits unwanted power with a spectrum emission mask (SEM). The mask is referenced by the total transmitted power or the maximum spectral density in the necessary bandwidth. In decibel units these are dBc and dBsd, respectively. The mask referenced by total transmitted power is

$$l_u(\Delta f)(c) = \frac{p_{ta}}{\Psi_u(\Delta f)} = \frac{p_{ta}}{\int_{-\infty}^{\infty} p_{ta}(f) |h_{ref}(f + \Delta f)|^2 df} \quad (\text{A-4})$$

where Δf is the difference between the transmit frequency, f_t , and the measurement frequency, f_m , p_{ta} is the total power at the antenna terminal, $p_{ta}(f)$ is the power spectral density at the antenna terminal, and Ψ_u is the unwanted power measured with a reference filter whose baseband impulse response is $h_{ref}(f)$.

Spurious attenuation is a special case of this mask. It is defined as the total power divided by the unwanted power measured with the reference filter centered at any frequency in the spurious domain

$$l_{spur} = \frac{p_{ta}}{\Psi_{ref}} \quad (\text{A-5})$$

The mask referenced by spectral density is

$$l_u(\Delta f)(sd) = \frac{\psi_n}{\Psi_u(\Delta f)} = \frac{\int_{-\infty}^{\infty} p_{ta}(f) |h_{ref}(f)|^2 df}{\int_{-\infty}^{\infty} p_{ta}(f) |h_{ref}(f + \Delta f)|^2 df} \quad (\text{A-6})$$

where ψ_n is the maximum power in the necessary bandwidth measured with the same reference filter as was used for the unwanted emissions.

The reference filter bandwidth is not necessarily the same in the OOB and spurious domains. Smaller bandwidths are necessary to accurately measure steep OOB attenuation. The OOB reference filter bandwidth is suggested to be on the order of 1% of the necessary bandwidth. The spurious reference filter bandwidth is dependent on carrier frequency. A 10 MHz bandwidth signal at 3000 MHz would use 100 kHz and 1 MHz for OOB and spurious measurement bandwidths, respectively.

The unwanted emission power can also be expressed in terms of effective isotropic radiated power (EIRP) in units of watts in the reference bandwidth

$$\zeta(\Delta f) = g_t \Psi_u(\Delta f) \quad (\text{A-7})$$

or in dB

$$Z(\Delta f)(\text{dB}) = G_t + \Psi_u(\Delta f) \quad (\text{A-8})$$

where $Z = 10 \log_{10} \zeta$, $G_t = 10 \log_{10} g_t$, and $\Psi_u = 10 \log_{10} \Psi_u$.

A.3 Received Unwanted Signal Power

The received power is

$$p_r = \int_{-\infty}^{\infty} p_r(f) df . \quad (\text{A-9})$$

Assuming antenna gains and propagation path loss are constant over the bandwidth of interest this expands to

$$p_r(d, \Delta f) = \frac{g_t g_r}{l_{cr} l_{pol} l_p(d)} \int_{-\infty}^{\infty} \frac{p_{tx}(f) |h_t(f)|^2 |h_r(f + \Delta f)|^2}{l_{ct}} df . \quad (\text{A-10})$$

Since

$$p_{ta}(f) = \frac{p_{tx}(f) |h_t(f)|^2}{l_{ct}} \quad (\text{A-11})$$

then

$$p_r(d, \Delta f) = \frac{g_t g_r}{l_{cr} l_{pol} l_p(d)} \int_{-\infty}^{\infty} p_{ta}(f) |h_r(f + \Delta f)|^2 df \quad (\text{A-12})$$

Defining frequency dependent rejection (FDR) [A-3] as the total power divided by the power after receiver filtering

$$l_{fdr}(\Delta f) = \frac{p_{ta}}{\int_{-\infty}^{\infty} p_{ta}(f) |h_r(f + \Delta f)|^2 df} \quad (\text{A-13})$$

where

$$p_{ta} = \int_{-\infty}^{\infty} p_{ta}(f) df \quad (\text{A-14})$$

then

$$p_r(d, \Delta f) = \frac{p_{ta} g_t g_r}{l_{cr} l_{pol} l_p(d) l_{fdr}(\Delta f)} \quad (\text{A-15})$$

In decibels the corresponding equation is

$$P_r(\Delta f) (dB) = P_{ta} + G_t + G_r - L_{cr} - L_{pol} - L_p(d) - L_{fdr}(\Delta f) \quad (\text{A-16})$$

A.4 Received Unwanted Signal Power in Terms of the Transmitted Unwanted Signal Power

The received power can also be written in terms of transmitted unwanted signal power. Dividing (A-13) by (A-4) and rearranging terms we find

$$l_{fdr}(\Delta f) = l_u(\Delta f) \frac{\int_{-\infty}^{\infty} p_{ta}(f) |h_{ref}(f + \Delta f)|^2 df}{\int_{-\infty}^{\infty} p_{ta}(f) |h_r(f + \Delta f)|^2 df} \quad (\text{A-17})$$

which can then be substituted in (A-16).

Furthermore if we assume Δf is in the spurious region and $p_{ta}(f)$ is constant across reference and radar filter bandwidths then

$$l_{fdr}(\Delta f) = l_{spur} \frac{b_{ref}}{b_r} \quad (\text{A-18})$$

where b_{ref} and b_r are the noise equivalent bandwidths defined as

$$b_{ref} = \int_{-\infty}^{\infty} |h_{ref}(f)|^2 df \quad (\text{A-19})$$

$$b_r = \int_{-\infty}^{\infty} |h_r(f)|^2 df \quad (\text{A-20})$$

or in dB

$$L_{fdr}(\Delta f) = L_{spur} + B_{ref} - B_r \quad (\text{A-21})$$

where $L_{fdr} = 10 \log_{10} l_{fdr}$, $L_{spur} = 10 \log_{10} l_{spur}$, $B_{ref} = 10 \log_{10} b_{ref}$, and $B_r = 10 \log_{10} b_r$.

Hence, the received power in the spurious region can be written in terms of spurious attenuation by

$$p_r = \frac{p_{ta} g_t g_r b_r}{l_{cr} l_{pol} l_p(d) l_{spur} b_{ref}} \quad (\text{A-22})$$

or in dB

$$P_r (dB) = P_{ta} + G_t + G_r - L_{cr} - L_{pol} - L_p(d) - L_{spur} - B_{ref} + B_r \quad (\text{A-23})$$

A.5 References

- [A-1] International Telecommunication Union, "Unwanted emissions in the out-of-band domain," Recommendation ITU-R SM.1541-4, September 2011.

- [A-2] International Telecommunication Union, “Unwanted emissions in the spurious domain,” Recommendation ITU-R SM.329-10, February 2003.
- [A-3] International Telecommunication Union, “Frequency and distance separations,” Recommendation ITU-R SM.337-6, 2008.

APPENDIX B: FAST METHOD FOR COMPUTING SEGMENTED, LOGNORMAL-DISTRIBUTION INTEGRAL

Interfering power from a cellular network is the sum of the powers or aggregate power of a set of base stations. If the power from each base station is log-normally distributed it can be demonstrated that the aggregate power of a moderate number of base stations is also log-normally distributed, especially in the range of 1 to 99 percent [B-1]. This is a pleasing result as it allows the use of the standard normal function or some variation of it such as the Q function to efficiently determine probabilities as follows. Let

$$I = \mu + Y = \mu + \sigma z \quad (\text{B-1})$$

where I is the aggregate quantile in dBW, μ is the mean or median in dBW, Y is the deviation, σ is the standard deviation in dBW, and z is the standard normal deviate

$$z = \frac{I - \mu}{\sigma} \quad (\text{B-2})$$

Then the probability density for I is

$$f(I) = \frac{1}{\sqrt{2\pi}\sigma} \exp\left(-\frac{(I - \mu)^2}{2\sigma^2}\right) \quad (\text{B-3})$$

The cumulative distribution function is

$$F(I) = \Pr\{J < I\} = \frac{1}{\sqrt{2\pi}\sigma} \int_{-\infty}^I \exp\left(-\frac{(X - \mu)^2}{2\sigma^2}\right) dX \quad (\text{B-4})$$

and the complementary cumulative distribution function is

$$1 - F(I) = \Pr\{J \geq I\} = \frac{1}{\sqrt{2\pi}\sigma} \int_I^{\infty} \exp\left(-\frac{(X - \mu)^2}{2\sigma^2}\right) dX \quad (\text{B-5})$$

Written in terms of z we have

$$\Pr\{Z < z\} = q = 1 - Q(z) \quad (\text{B-6})$$

and

$$\Pr\{Z \geq z\} = 1 - q = Q(z) \quad (\text{B-7})$$

where

$$Q(z) = \frac{1}{\sqrt{2\pi}} \int_z^{\infty} e^{-t^2/2} dt \quad (\text{B-8})$$

However, if the power from each base station is not log-normal, as is the case for the maritime propagation channel, the aggregate power may not be log-normal and we must look for another method to efficiently determine probabilities.

Inspired by the method used by ITM to model the propagation loss distribution with fading, enhancement, and ducting regions using 3 log-normal segments we divide the aggregate power distribution acquired through Monte Carlo analysis into $2K$ log-normal segments. The segments and their parameters are designated by the subscript k . Parameters associated with the median are designated by the subscript med .

In the case of the k -th linear segment with probabilities $q_{k-1} < q < q_k$ the aggregate power is

$$I = \mu_k + \sigma_k z \quad (\text{B-9})$$

The segment standard deviations are

$$\sigma_k = \frac{I_k - I_{med}}{z_k - z_{med}} = \frac{I_k - I_{med}}{z_k} \quad (\text{B-10})$$

The segment means for the fading side of the distribution are computed from K to 2 with the approximation $\mu_{K+1} = \mu_{med}$

$$\mu_k = \mu_{k+1} + z_k(\sigma_k - \sigma_{k-1}). \quad (\text{B-11})$$

The segment means for the enhancement side of the distribution are computed from $K+3$ to $2K+1$ with the approximation $\mu_{K+2} = \mu_{med}$

$$\mu_k = \mu_{k-1} + z_{k-2}(\sigma_{k-2} - \sigma_{k-1}). \quad (\text{B-12})$$

The resulting mean vector indices are then decremented by one, yielding the vector

$$\mu_k, k \in \{1, 2, \dots, 2K\}. \quad (\text{B-13})$$

We can now characterize the aggregate distribution function with σ_k and μ_k calculated at specific probabilities, q_k , and the corresponding standard normal deviates, z_k . Through trial and error, we found satisfactory agreement with $K = 13$. The $2K = 26$ segments are delineated in Table B-1.

Table B-1. Probability, q_k , and corresponding standard normal deviate, z_k , for the each of the 26 segments in the aggregate distribution function.

k	q_k	z_k	k	q_k	z_k
1	0.001	-3.090	14	0.60	0.253
2	0.002	-2.878	15	0.70	0.524
3	0.005	-2.576	16	0.80	0.841
4	0.01	-2.327	17	0.85	1.036
5	0.02	-2.054	18	0.90	1.282

k	q_k	z_k	k	q_k	z_k
6	0.04	-1.751	19	0.93	1.476
7	0.05	-1.645	20	0.95	1.645
8	0.07	-1.476	21	0.96	1.751
9	0.1	-1.282	22	0.98	2.054
10	0.15	-1.036	23	0.99	2.327
11	0.20	-0.841	24	0.995	2.576
12	0.30	-0.524	25	0.998	2.878
13	0.40	-0.253	26	0.999	3.090

B.1 References

- [B-1] S. C. Schwartz and Y. S. Yeh, "On the Distribution Function and Moments of Power Sums With Log-Normal Components," Bell System Technical Journal, Vol. 61, #7, pp. 1441-1462, Sept. 1982.

APPENDIX C: RISE IN NOISE POWER

In this section we calculate the rise in noise power relative to receiver noise power when an interferer with Gaussian noise characteristics is received.

Let the rise in noise power relative to receiver noise power be

$$y = \frac{i + n}{n} = i/n + 1 \quad (\text{C-1})$$

where i is the interfering signal power and n is the receiver noise power.

Let $u = i/n$ and $U = 10 \log_{10} u$ then

$$y = 10^{U/10} + 1 \quad (\text{C-2})$$

so that the rise in dB is

$$Y = \log_{10} \left(10^{U/10} + 1 \right) \text{ (dB)} \quad (\text{C-3})$$

Results are plotted below. INR of -6, -9, and -12 corresponds to an approximate 1, 0.5, and 0.25 dB rise in power.

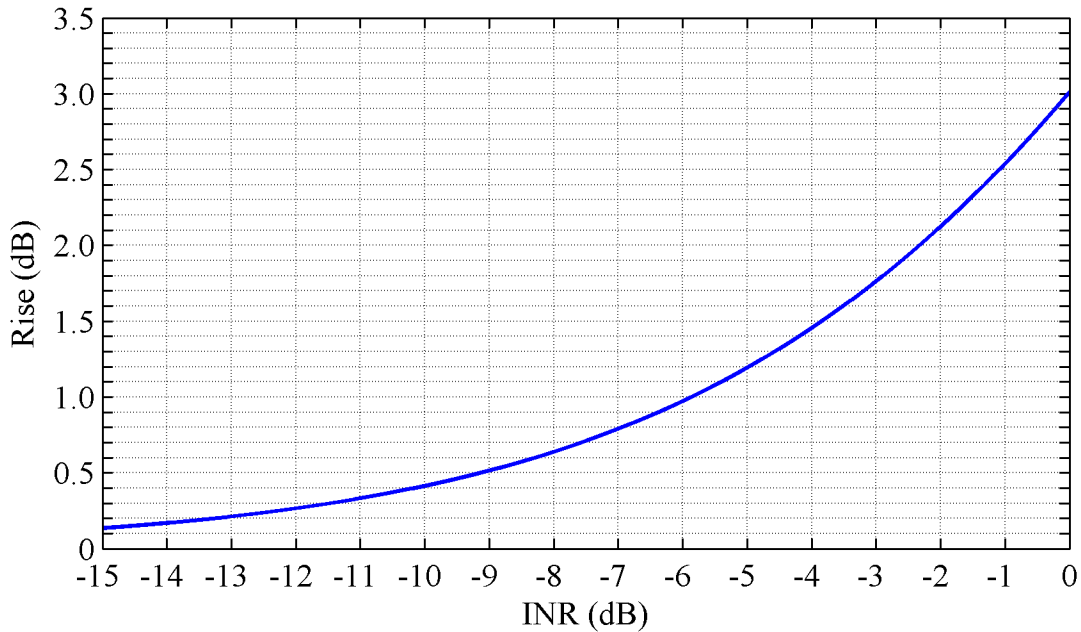


Figure C-1. Rise in noise power relative to receiver noise power for interfering signal with Gaussian noise characteristics.

APPENDIX D: EMISSION LIMITS

D.1 ITU-R Spurious Emission Limit

The following analysis calculates the BRS maximum spurious emission attenuation and spurious effective isotropic radiated power (EIRP) according to ITU-R guidelines which are summarized in [D-1]. Related documents are [D-2] and [D-3].

Spurious emissions are defined by the ITU-R as “emissions in the spurious domain which consists of frequencies separated from the center frequency of the emission by 250% or more of the necessary bandwidth”.

General spurious emission limits are specified as attenuation below the power supplied to the antenna transmission line in Category A tables. More restrictive emission limits for the United States are specified in Category C tables. If the service is not addressed in Category C, limits in Category A are used.

Spurious emission attenuation is

$$l_{spur} = \frac{p_t}{\Psi_{ref}} \quad (D-1)$$

where p_t is the total transmitted power and Ψ_{ref} is the spurious power at the transmitter antenna input measured in the ITU reference equivalent noise bandwidth, b_{ref} . In dB we have

$$L_{spur}(dB) = P_t - \Psi_{ref} \quad (D-2)$$

where $L_{spur} = 10 \log_{10} l_{spur}$, $P_t = 10 \log_{10} p_t$, $\Psi_{ref} = 10 \log_{10} \Psi_{ref}$.

Spurious EIRP is

$$\zeta_{ref} = \Psi_{ref} g \quad (D-3)$$

where g is the transmitting antenna gain. In dB we have

$$Z_{ref}(dB) = \Psi_{ref} + G \quad (D-4)$$

where $Z_{ref} = 10 \log_{10} \zeta_{ref}$ and $G = 10 \log_{10} g$.

Combining the two expressions we have

$$Z_{ref}(dB) = P_t - L_{spur} + G \quad (D-5)$$

Category C does not address the limit for the BRS service. Consequently the limit in Category A is used, i.e.,

$$L_{spur}(dB) = 43 + P_t \quad (D-6)$$

where P_t is in dBW or 70 dBc, whichever is less stringent. In this case, the former is less stringent. The b_{ref} is 1 MHz for frequencies greater than 1 GHz.

Table D-1. ITU-R Spurious emission power limit for BRS base station.

Parameter	Value	Calculation
P_t	20 watts for 10 MHz bandwidth signal	43 dBm
L_{spur}	56 dB	-56
Ψ_{ref}		-13 dBm/1 MHz
G	15 dB	+15
Z_{ref}		+2 dBm/1 MHz

D.2 ETSI Spectrum Emission Mask

Table D-2 shows the ETSI SEM limits [D-4] for the BRS emissions in the operating band. The operating band is the spectrum 10 MHz above and below the allocated spectrum lower and upper edges, respectively. The SEM is defined terms of Δf and f_{offset} . These are defined as:

- f_{offset} is the separation between the allocated spectrum edge and the measurement filter center frequency
- $f_{offset_{max}}$ is the separation between the allocated spectrum edge and the operating band edge
- Δf is separation between the allocated spectrum edge and the closest measurement filter -3 dB point
- Δf_{max} is $f_{offset_{max}}$ minus one-half the measurement filter 3 dB bandwidth

Figure D-1 displays these limits in a 30 kHz bandwidth for the 2500–2700 MHz allocated spectrum along with the -52 dBm/MHz (or -67.2 dBm/30 kHz) limit outside the allocated spectrum [D-5]. The limits assume a 10 MHz bandwidth signal next to the band edge with 20 W transmission power.

Table D-2 Spectrum emission mask breakpoints.

Δf (MHz)	f_{offset} (MHz)	SEM	SEM units
$0 \leq \Delta f < 0.200$	$0.15 \leq f_{offset} < 0.215$	-14	dBm/30 kHz
$0.200 \leq \Delta f < 1.0$	$0.215 \leq f_{offset} < 1.015$	$-14 - 15(\Delta f - 0.200)$	dBm/30 kHz
Not needed	$1.015 \leq f_{offset} < 1.5$	-26	dBm/30 kHz
$1 \leq \Delta f \leq \text{Min}(\Delta f_{max}, 10)$	$1.5 \leq f_{offset} < \text{Min}(f_{offset_{max}}, 10.5)$	-13	dBm/1 MHz
$10 \leq \Delta f \leq \Delta f_{max}$	$10.5 \leq f_{offset} < f_{offset_{max}}$	-15	dBm/1 MHz

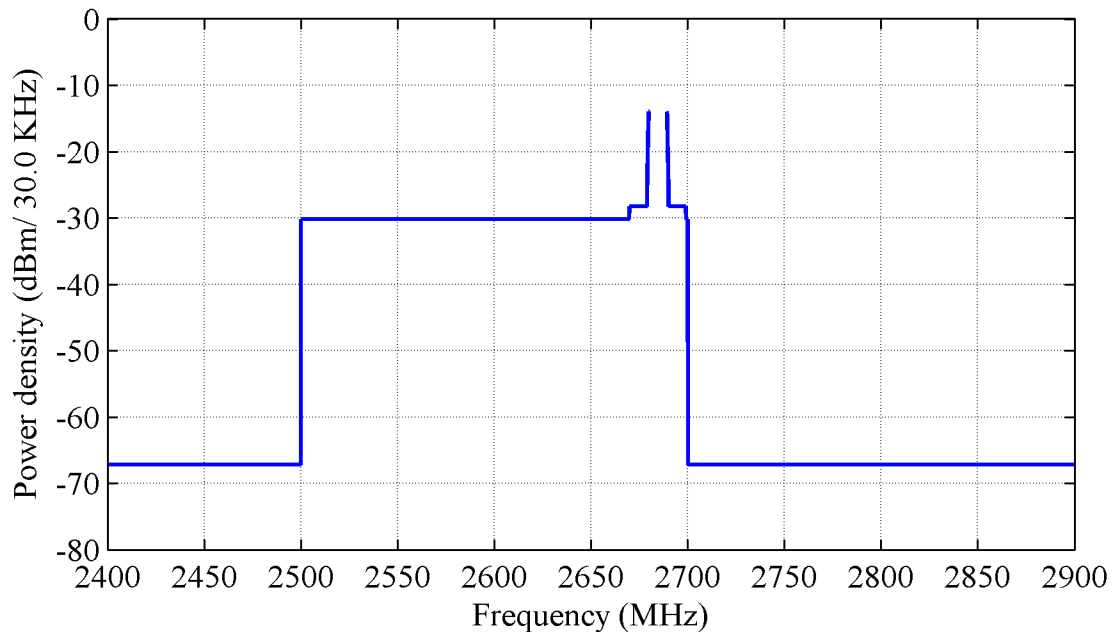


Figure D-1. 3GPP spectrum emission mask in 30.0 kHz bandwidth.

D.3 References

- [D-1] International Telecommunication Union, “Unwanted emissions in the spurious domain,” Recommendation ITU-R SM.329-10, February 2003.
- [D-2] International Telecommunication Union, “Generic unwanted emission characteristics of base stations using the terrestrial radio interfaces of IMT-2000,” Recommendation ITU-R M.1580-3, October 2009.
- [D-3] International Telecommunication Union, “Generic unwanted emission characteristics of mobile stations using the terrestrial radio interfaces of IMT-2000,” Recommendation ITU-R M.1581-3, October 2009.
- [D-4] European Telecommunications Standards Institute 3rd Generation Partnership Project, ETSI TS 137 104 V11.2.1 (2012-10), “Digital Cellular Telecommunications System (Phase 2+); Universal Mobile Telecommunications System (UMTS); LTE; E-UTRA, UTRA, and GSM/EDGE; Multistandard Radio Base Station (BS) radio transmission and reception (3GPP TS 37.104 version 11.2.1 Release 11),” Table 6.6.2.1-1, p. 37.
- [D-5] European Telecommunications Standards Institute 3rd Generation Partnership Project, ETSI TS 137 104 V11.2.1 (2012-10), “Digital Cellular Telecommunications System (Phase 2+); Universal Mobile Telecommunications System (UMTS); LTE; E-UTRA, UTRA, and GSM/EDGE; Multistandard Radio Base Station (BS) radio transmission and reception (3GPP TS 37.104 version 11.2.1 Release 11),” Table 6.6.1.3.1-1, pp. 30-33.

APPENDIX E: VARIABLE SNR DATA EXAMPLES

This Appendix shows raw variable SNR reliability data for two IEC 62388 standard cases. Case 1 is a 60 m high shoreline 37 km away. Case 6 is a small boat with a reflector 6.8 km away. Case 1 signal and interference powers have a considerable amount of variability. Case 6 signal and interference powers are relatively constant.

Reliability is a function of radar to target range and separation distance. Figures E-1 and E-2 show reliability over a range of separation distances when radar to target range is fixed. Figures E-3 and E-4 show reliability over radar to target ranges when the separation distance is fixed. All calculations are done with an INR of -6 dB and an RCS that has been reduced by the 99% power margin.

Figure E-1 shows that Case 1 needs less than 56 dB spurious attenuation at 90% reliability when the separation distance is 38 km and the radar to target range is 37 km. This corresponds with Figure E-3 which shows reliability close to 1 when spurious attenuation is 56 dB or more at these same distances. Figure E-2 shows that Case 6 needs 77.9 dB spurious attenuation at 90% reliability when the separation distance is 7.8 km and the radar to target range is 6.8 km. This corresponds to Figure E-4 which shows that 90% reliability can be obtained with spurious attenuations greater than 75 dB at these same distances.

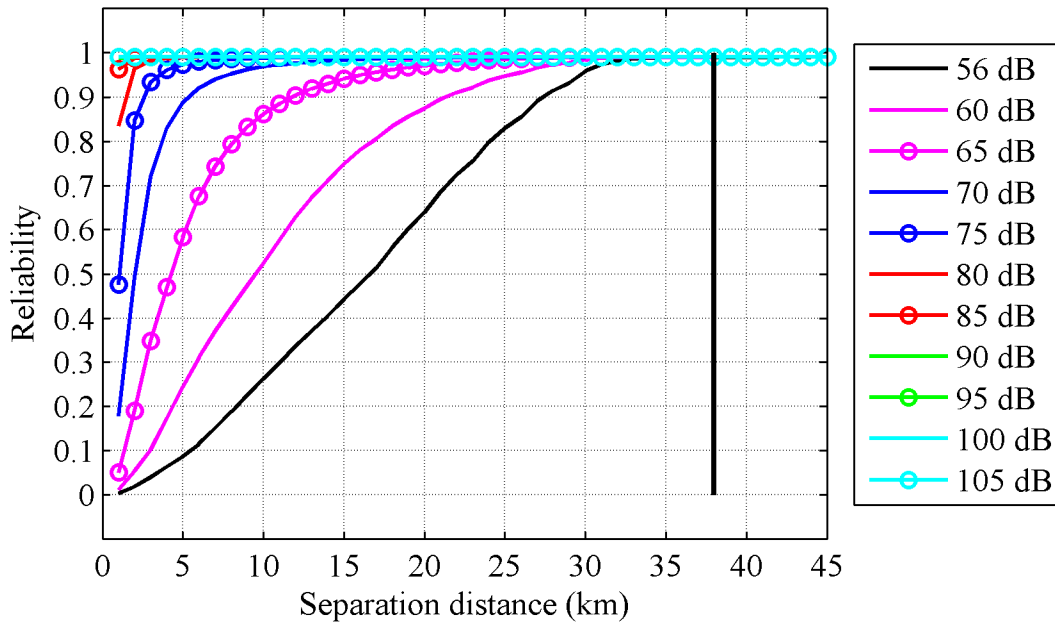


Figure E-1. Case 1 reliability as a function of separation distance. The thick vertical black line at 38.0 km is the separation distance used in our analysis. Reliabilities for spurious attenuations above 85 dB are approximately 1.0 for all separation distances.

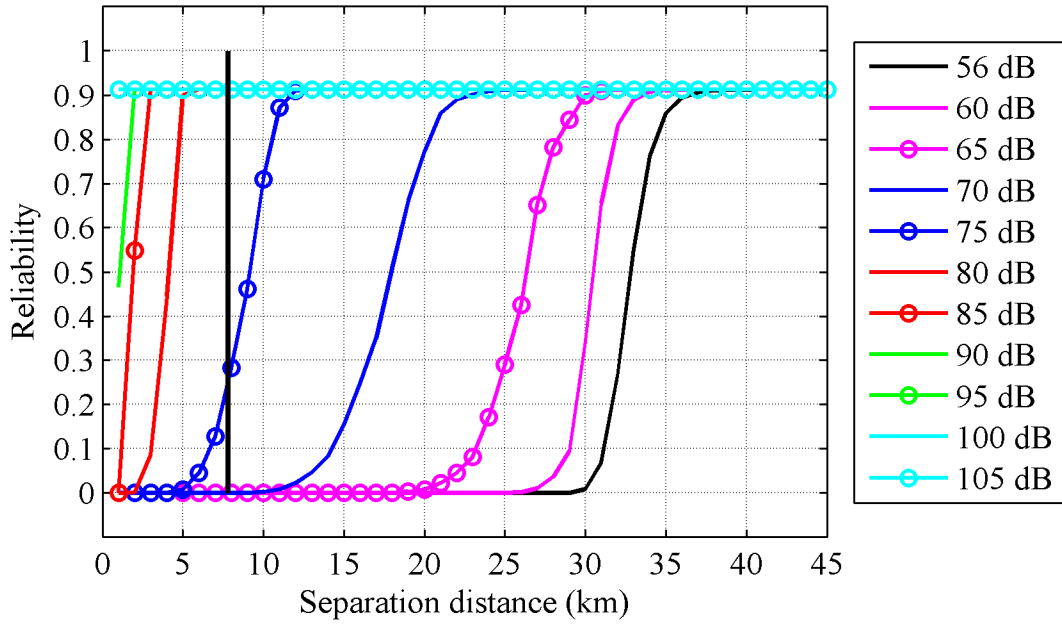


Figure E-2. Case 6 reliability as a function of separation distance. The thick vertical black line at 7.8 km is the separation distance used in our analysis. Reliabilities for spurious attenuations above 90 dB are approximately 1.0 for all separation distances.

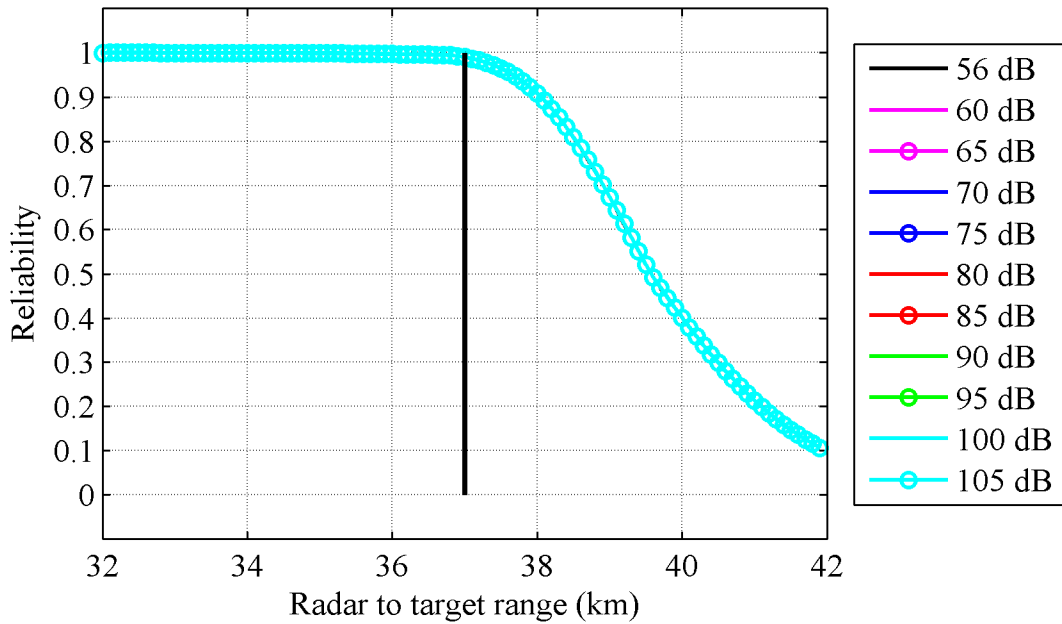


Figure E-3. Case 1 reliability as a function of radar to target range. The thick vertical black line at 37.0 km is the radar to target range used in our analysis. All spurious attenuation curves lie on top of each other.

APPENDIX F: WIMAX MEASURED PSD AND FILTERED PSD

F.1 PSD Measurement

The PSD of a BRS WiMAX BS operating in the 2500–2700 MHz band was measured in a laboratory with a spectrum analyzer as described in the previous background report [F-1]. Figure F-1 shows the results of this measurement in terms of power at the measurement system input. The measurement was performed with a 1 MHz frequency step and 100 kHz resolution bandwidth. The center frequency and bandwidth are estimated to be 2683.5 MHz and 9.3 MHz, respectively. The measurement system noise figure was 15.2 dB. A horizontal line has also been added at -108.8 dBm to demark the measurement system noise floor.

The signal is occupying a 10 MHz BRS channel adjacent to the lower edge of the 2700–2900 radar band and has unwanted emissions above and below the BRS channel. The unwanted emissions below the BRS channel fall to approximately -90 dBm by 2640 MHz then level off until 2450 MHz where they reach the measurement system noise floor. Unwanted emissions above the BRS channel fall to the noise floor by 2760 MHz.

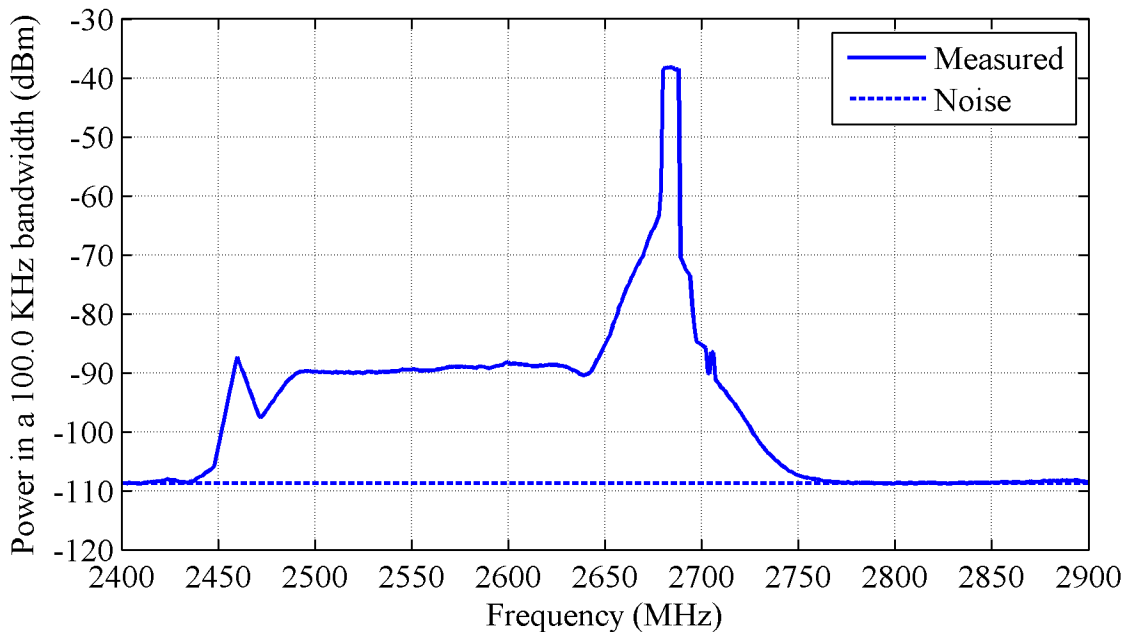


Figure F-1. PSD measurement

F.2 Filtered PSD Measurement

The filtered PSD was created by filtering the measured PSD. The filter was designed to be attached at the BRS base station antenna input and attenuate unwanted emissions in adjacent bands. Filter specifications are provided in Table F-1. Filtering was done analytically in the

frequency domain. Figure F-2 shows the measured filter frequency response. Figure F-3 shows the measured PSD before and after filtering.

Table F-1. Transmitter filter specifications.

Specification	Value	Note
Manufacturer	K&L Microwave Inc.	Salisbury, MD USA
Part Number	WSF-00543	
Passband	2500-2692 MHz	
Insertion Loss	1.50 dB max	
Return Loss	18.0 dB min	
Amplitude Flatness	+/- 0.75 dB max	
Stop Bands	0-2375 and 2704-4000 MHz	
Rejection	55 dB min	

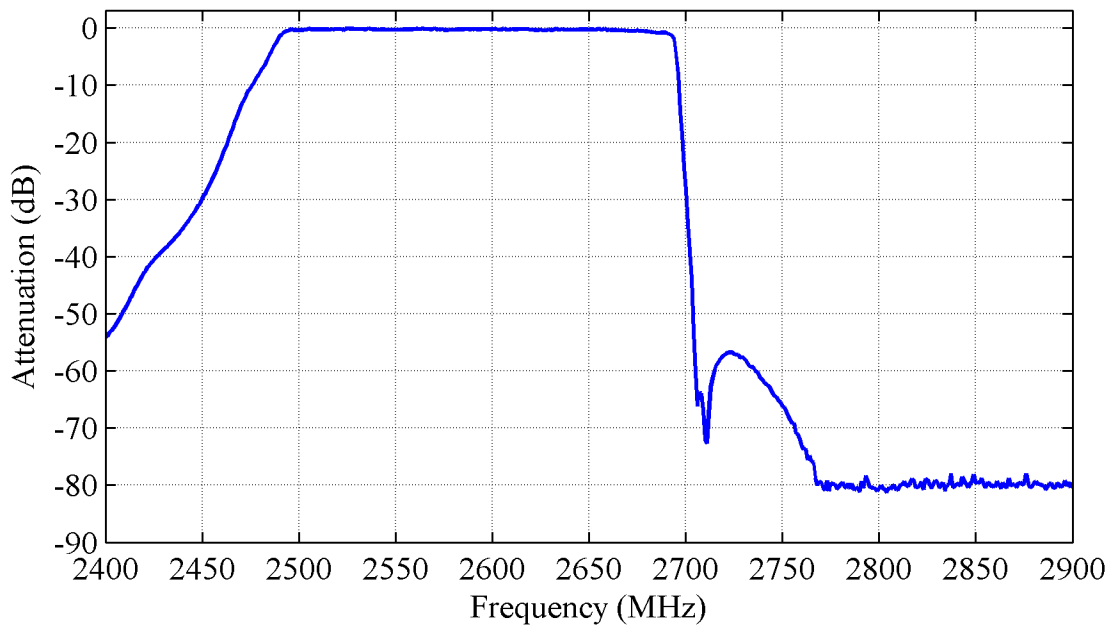


Figure F-2. Transmitter filter frequency response.

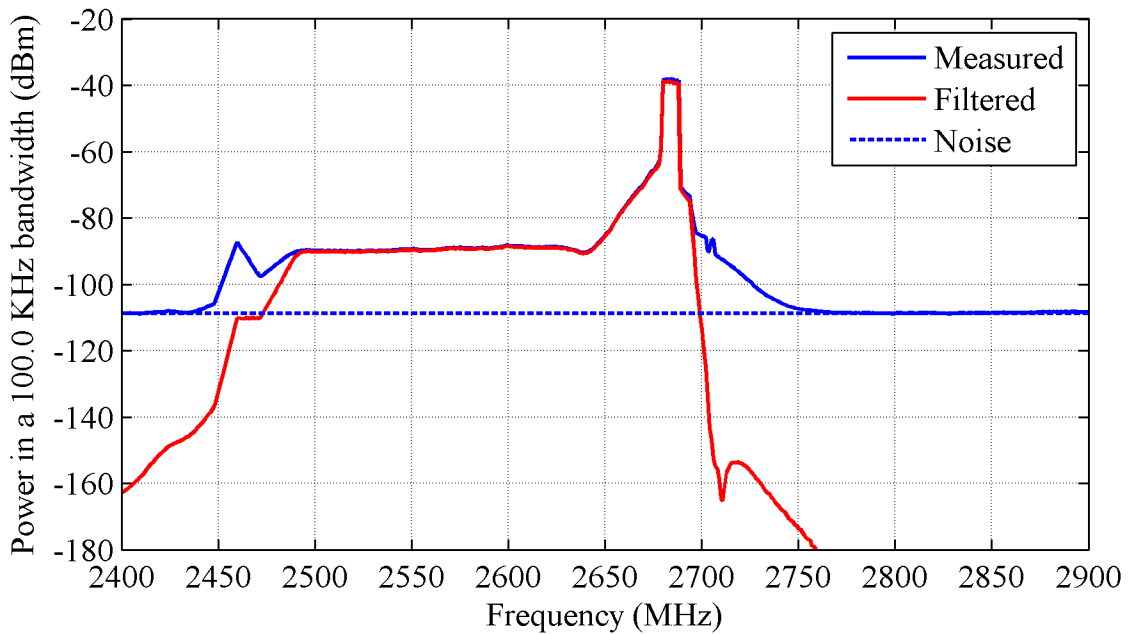


Figure F-3. Measured and filtered PSDs.

F.3 References

- [F-1] R. Achatz, P. McKenna, R. Dalke, N. DeMinco, F. Sanders, and J. Carroll, “Effect of broadband radio service reallocation on 2900–3100 MHz band marine radars: Background,” NTIA Report TR-15-513, April 2015. <http://www.its.bldrdoc.gov/publications/2795.aspx>

APPENDIX G: RADAR IF FILTER FREQUENCY RESPONSES

Radar IF filter frequency response measurements of two magnetron 2900–3100 MHz band maritime radars, identified as Radar A and Radar C, are described in this Appendix. The filters were measured to characterize radars during interference tests [G-1]. Each radar had two IF filters corresponding to short and long pulse widths.

The measurement configuration consisted of a signal generator that provided a continuous wave test signal, the radar, and a spectrum analyzer that measured the response to the test signal. The signal was injected into the radar front-end input rather than the IF input. This restricted the measurement dynamic range to approximately 60 dB. The spectrum analyzer was attached to receiver IF filter output. Radar A measurement consisted of 600 points measured with a 150 kHz spacing, 100 kHz bandwidth, and 0.3 s dwell time. Radar C measurement consisted of 1000 points measured with a 164 kHz spacing, 100 kHz bandwidth, and 0.0492 s dwell time.

Figures G-1 and G-2 show the results of these measurements along with the frequency responses of ideal filters that roll off at a rate of 80 dB/decade below the -3 dB points [G-2]. While the ideal filter frequency response does not match that of the long pulse, it does match that of the short pulse in all but the higher frequencies of Radar C, which falls off at approximately 40 dB/decade. Since 80 dB/decade is achievable in most circumstances, we conclude that the frequency response of the short pulse filter can be reasonably replaced by an ideal filter that falls off at a rate of 80 dB/decade.

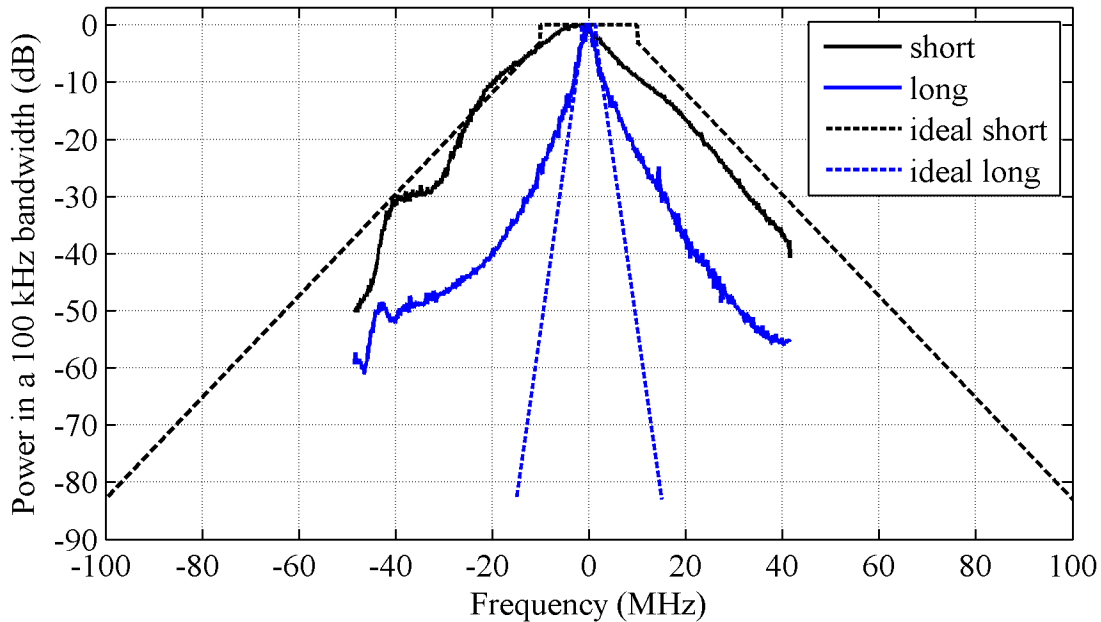


Figure G-1. Radar A measured and ideal, long and short pulse IF filter frequency responses.

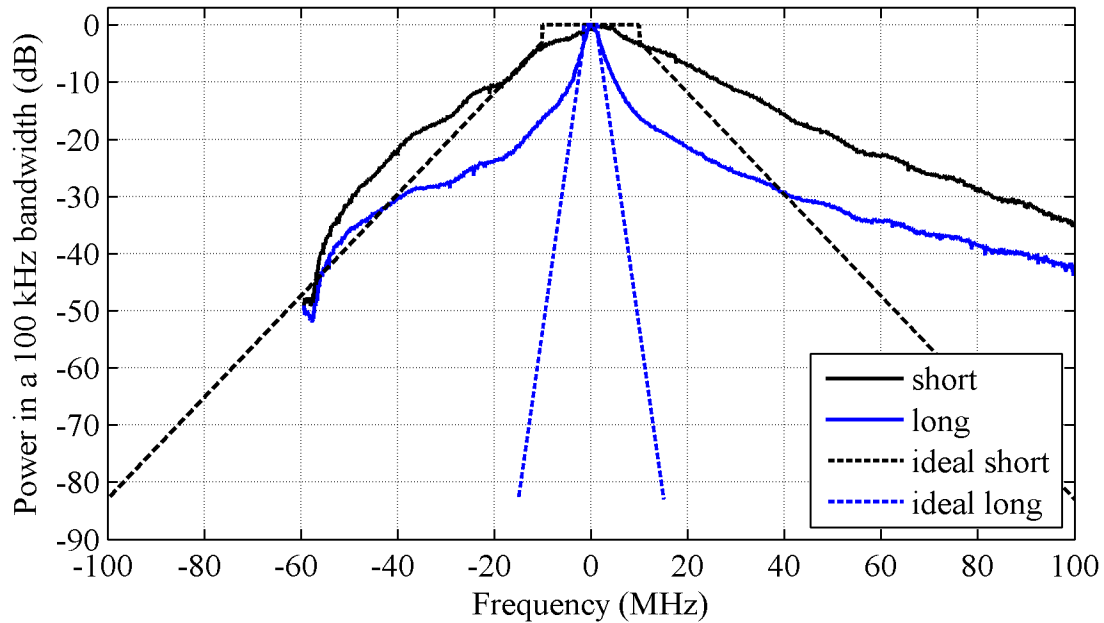


Figure G-2. Radar C measured and ideal, long and short pulse IF filter frequency responses.

G.1 References

- [G-1] F. Sanders et. al., “Effects of RF interference on radar receivers,” NTIA Report TR-06-444, September 2006, <http://www.its.bldrdoc.gov/publications/2481.aspx>.
- [G-2] International Telecommunication Union, “Procedures for determining the potential for interference between radars operating in the radio determination service and systems in other services,” ITU-R Recommendation M.1461-1, June 2003, p. 9.

APPENDIX H: RESULTS FOR OTHER INR

H.1 Results for -9 dB INR

Table H-1. Separation distance results for -9.0 dB allowable INR and 2.7% allowable degradation.

Parameter			Separation distance, d_{min} (km)						
L_{spur}	Ψ_{spur}	Z_{itu}	ITM 50%	ITM 60%	ITM 70%	ITM 80%	ITM 90%	ITM 95%	ITM 99%
dB	dBm/MHz	dBm/MHz							
56	-13	2	35.4	35.7	36.2	36.7	37.7	38.8	42.2
60	-17	-2	33.0	33.3	33.6	34.0	34.8	35.7	37.9
65	-22	-7	30.0	30.3	30.6	30.9	31.5	32.2	33.9
70	-27	-12	25.4	25.9	26.2	26.7	27.6	28.9	30.2
75	-32	-17	16.6	16.9	17.2	17.6	18.3	19.1	20.9
80	-37	-22	8.1	8.2	8.3	8.4	8.5	8.7	9.0
85	-42	-27	3.6	3.6	3.6	3.7	3.7	3.7	3.7
90	-47	-32	1.7	1.7	1.7	1.7	1.7	1.7	1.7
95	-52	-37	< 1	< 1	< 1	< 1	< 1	< 1	< 1

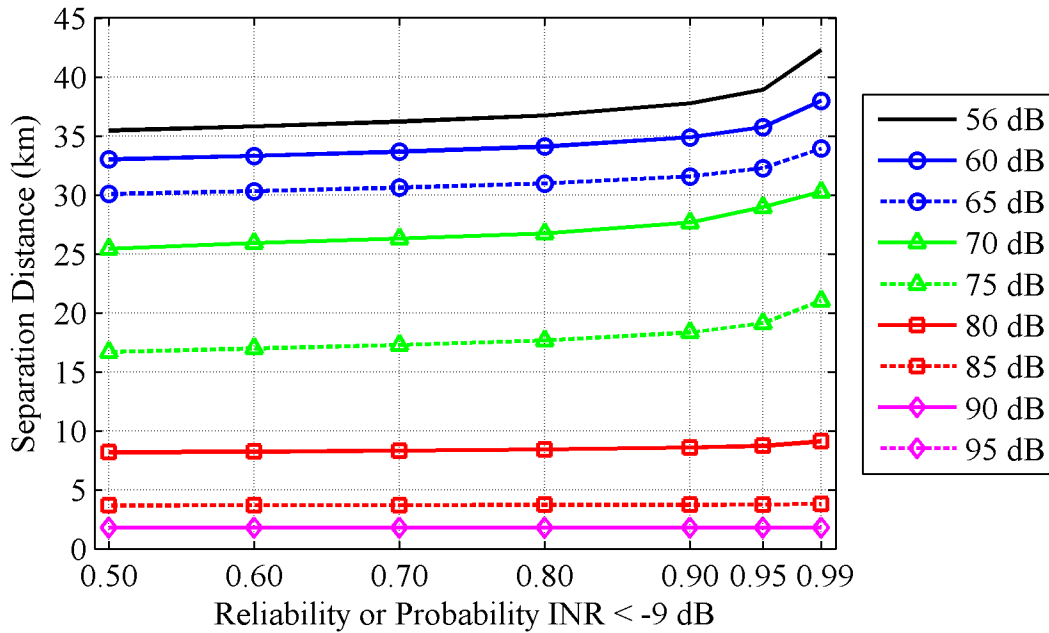


Figure H-1. Separation distance versus reliability for -9 dB INR. 95 dB attenuation produces separation distances less than the 1 km propagation model limit and is not shown.

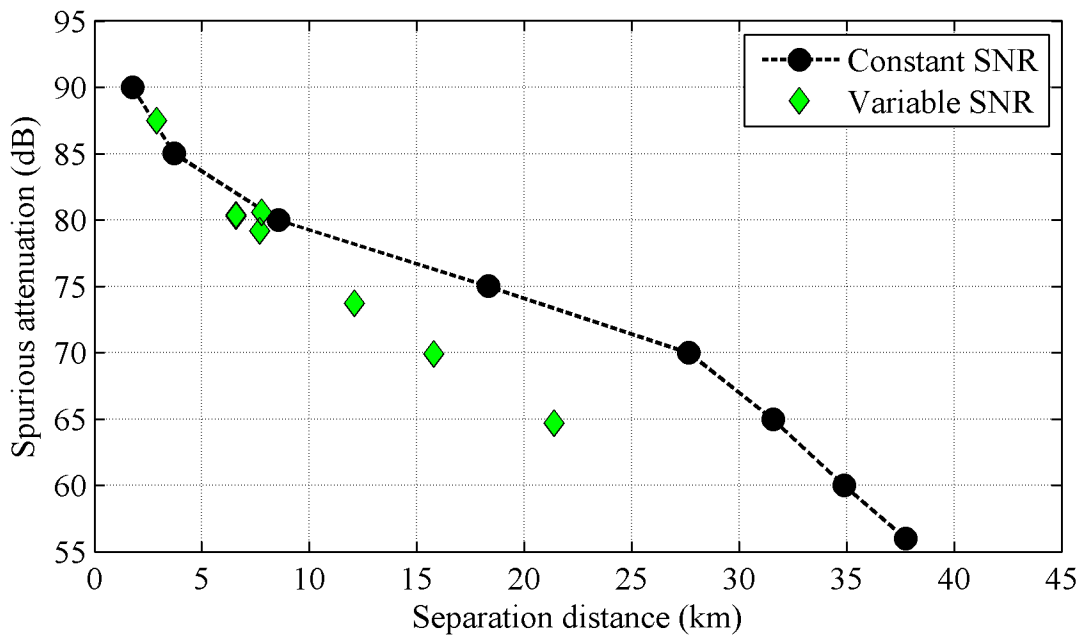


Figure H-2. Spurious attenuation for IEC 62388 standard clutter free test cases with -9 dB INR using constant and variable SNR for 90% reliability.

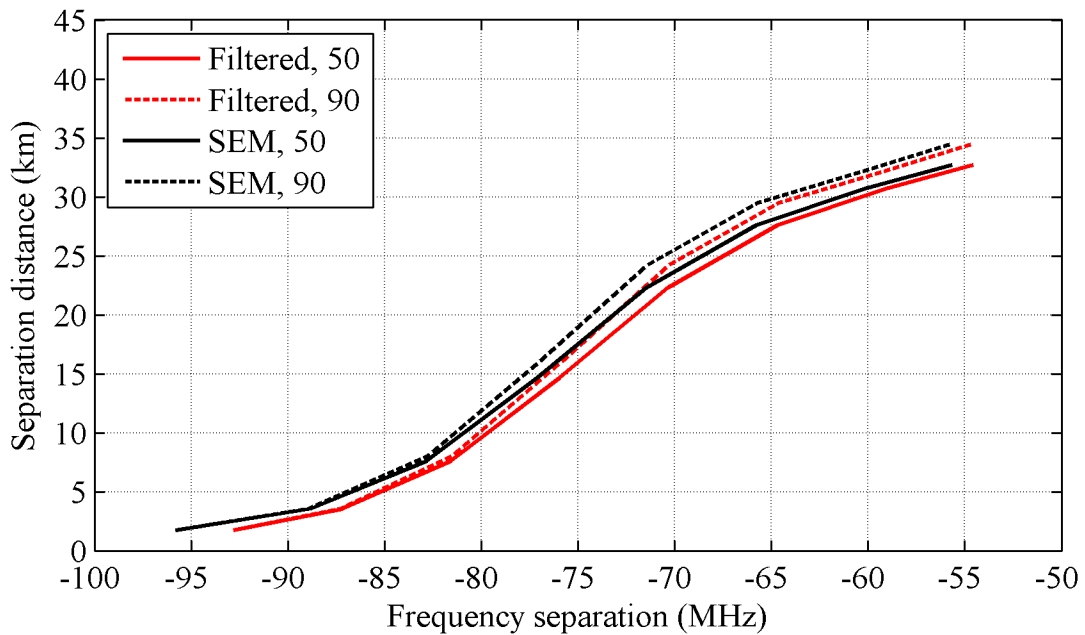


Figure H-3. Separation distance versus frequency separation for 50 and 90% reliability -9 dB INR with 20 MHz radar detection IF bandwidth.

H.2 Results for -12 dB INR

Table H-2. Separation distance results for -12.0 dB allowable INR and 1.4% allowable degradation.

Parameter			Separation distance, d_{min} (km)						
L_{spur}	Ψ_{spur}	Z_{itu}	ITM	ITM	ITM	ITM	ITM	ITM	ITM
dB	dBm/MHz	dBm/MHz	50%	60%	70%	80%	90%	95%	99%
56	-13	2	37.3	37.7	38.2	38.8	40.1	41.7	46.0
60	-17	-2	34.8	35.1	35.5	36.0	37.0	38.0	41.0
65	-22	-7	31.8	32.0	32.4	32.8	33.5	34.3	36.2
70	-27	-12	28.8	29.1	29.4	29.7	30.3	30.9	32.4
75	-32	-17	22.2	22.2	23.1	23.6	24.6	26.0	28.3
80	-37	-22	12.8	13.0	13.2	13.5	14.0	14.4	15.5
85	-42	-27	5.9	5.9	5.9	6.0	6.0	6.1	6.3
90	-47	-32	2.7	2.7	2.7	2.7	2.7	2.7	2.7
95	-52	-37	1.3	1.3	1.3	1.3	1.3	1.3	1.3
100	-57	-42	< 1	< 1	< 1	< 1	< 1	< 1	< 1

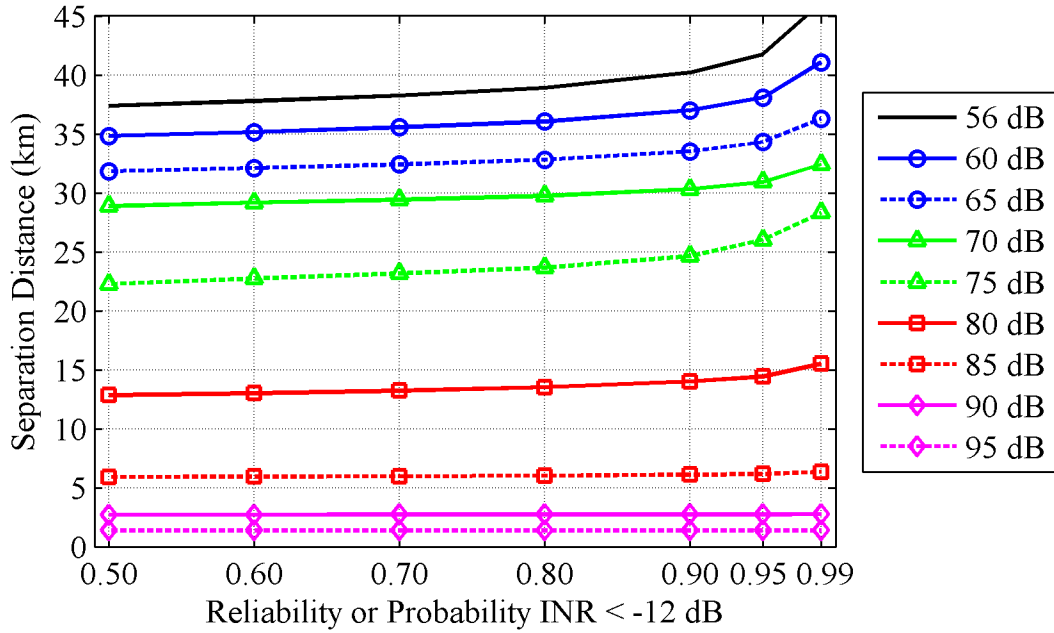


Figure H-4. Separation distance versus reliability for -12 dB INR.

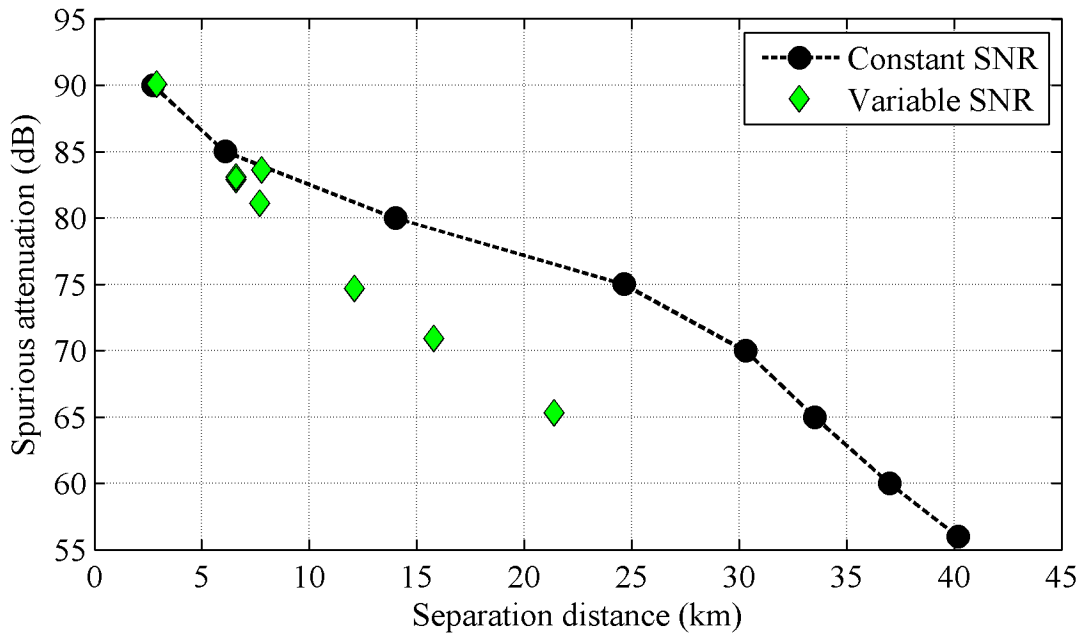


Figure H-5. Spurious attenuation for IEC 62388 standard clutter free test cases with -12 dB INR using constant and variable SNR for 90% reliability.

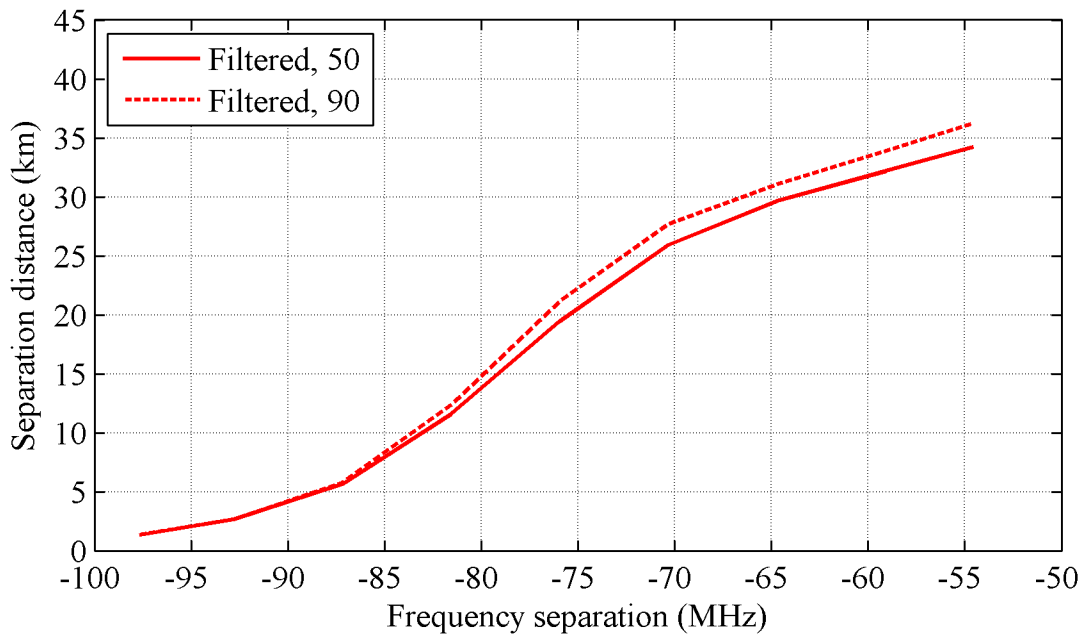


Figure H-6. Separation distance versus frequency separation for 50 and 90% reliability -12 dB INR with 20 MHz radar detection IF bandwidth.

APPENDIX I: PROBABILITY

The cumulative distribution function is

$$F(x) = \Pr\{\mathcal{X} < x\} = \int_{-\infty}^x f(z)dz \quad (\text{I-1})$$

where \mathcal{X} is a random variable. A specific probability between 0 and 1 is expressed as $\Pr\{\mathcal{X} < x_0\}$.

The inverse of the cumulative distribution function is the complementary cumulative distribution function

$$F'(x) = \Pr\{\mathcal{X} \geq x\} = 1 - F(x) \quad (\text{I-2})$$

The probability density function is

$$f(x) = \frac{dF(x)}{dx} \quad (\text{I-3})$$

If a change in variables is made such as $y = g(x)$ the following relation is true

$$f(x)dx = f(y)dy \quad (\text{I-4})$$

The joint cumulative distribution of two random variables is

$$F(x, y) = \Pr\{\mathcal{X} < x, \mathcal{Y} < y\} \quad (\text{I-5})$$

The joint probability density function is

$$f(x, y) = \frac{\partial^2 F(x, y)}{\partial x \partial y} \quad (\text{I-6})$$

which can also be expressed in terms of the product of the conditional probability density function and the probability density function of the other random variable

$$f(x, y) = f(x|y)f(y) = f(y|x)f(x) \quad (\text{I-7})$$

BIBLIOGRAPHIC DATA SHEET

1. PUBLICATION NO. TR-15-514	2. Government Accession No.	3. Recipient's Accession No.
4. TITLE AND SUBTITLE Effect of Broadband Radio Service Reallocation on 2900–3100 MHz Band Marine Radars: Unwanted Emissions		5. Publication Date April 2015
		6. Performing Organization Code NTIA/ITS.T
7. AUTHOR(S) Robert Achatz, Paul McKenna, Roger Dalke, Frank Sanders		9. Project/Task/Work Unit No. 3105011-300
		10. Contract/Grant Number.
8. PERFORMING ORGANIZATION NAME AND ADDRESS Institute for Telecommunication Sciences National Telecommunications & Information Administration U.S. Department of Commerce 325 Broadway Boulder, CO 80305		12. Type of Report and Period Covered
11. Sponsoring Organization Name and Address U.S. Coast Guard Spectrum Management Telecommunications Policy Division U.S. Coast Guard CG-652, 2100 2 nd St. SW Stop 7101 Washington, DC 20593-7101		
14. SUPPLEMENTARY NOTES		
15. ABSTRACT (A 200-word or less factual summary of most significant information. If document includes a significant bibliography or literature survey, mention it here.) Spectrum reallocations may place broadband radio services (BRS) near spectrum used by 2900–3100 MHz band marine radars. Signals from the BRS base stations can potentially introduce unwanted emissions in the radar detection bandwidth and cause interference. Interference protection criteria (IPC) are needed to mitigate this effect. The primary IPC of concern are the interference to noise power ratio (INR) and the reliability of the radar link at a specified radar signal to noise power ratio (SNR). Reliability is determined by radio wave propagation path loss variability which increases with distance. Distance separation between base stations and radar for various spurious attenuations were calculated using reliability expressions for short radar to target ranges with constant SNR and for longer radar to target ranges with variable SNR. For a magnetron radar under clutter free conditions, 90 dB of spurious attenuation is needed to obtain 90% radar operational reliability at 1.2 km when the INR is -6 dB and the SNR is constant. Reducing the INR to -9 and -12 dB increased the separation distance to 1.7 and 2.7 km, respectively. At longer base station to radar separation distances, variable SNR required less spurious attenuation than constant SNR. Consequently, constant SNR analysis can be considered worst case. Distance and frequency separation were calculated using frequency dependent rejection (FDR). These calculations showed that for constant SNR 92.8 MHz of frequency separation is required to meet the 90% reliability IPC at 1.2 km separation distance when the INR is -6 dB. Only 54.6 MHz frequency separation is needed when the separation distance is increased to 32.8 km.		
16. Key Words (Alphabetical order, separated by semicolons) broadband radio service, interference, interference protection criteria, marine radar, radar, radio wave propagation, radio spectrum engineering, spurious emissions		
17. AVAILABILITY STATEMENT <input checked="" type="checkbox"/> UNLIMITED. <input type="checkbox"/> FOR OFFICIAL DISTRIBUTION.	18. Security Class. (This report) Unclassified	20. Number of pages
	19. Security Class. (This page) Unclassified	21. Price:

NTIA FORMAL PUBLICATION SERIES

NTIA MONOGRAPH (MG)

A scholarly, professionally oriented publication dealing with state-of-the-art research or an authoritative treatment of a broad area. Expected to have long-lasting value.

NTIA SPECIAL PUBLICATION (SP)

Conference proceedings, bibliographies, selected speeches, course and instructional materials, directories, and major studies mandated by Congress.

NTIA REPORT (TR)

Important contributions to existing knowledge of less breadth than a monograph, such as results of completed projects and major activities.

JOINT NTIA/OTHER-AGENCY REPORT (JR)

This report receives both local NTIA and other agency review. Both agencies' logos and report series numbering appear on the cover.

NTIA SOFTWARE & DATA PRODUCTS (SD)

Software such as programs, test data, and sound/video files. This series can be used to transfer technology to U.S. industry.

NTIA HANDBOOK (HB)

Information pertaining to technical procedures, reference and data guides, and formal user's manuals that are expected to be pertinent for a long time.

NTIA TECHNICAL MEMORANDUM (TM)

Technical information typically of less breadth than an NTIA Report. The series includes data, preliminary project results, and information for a specific, limited audience.

For information about NTIA publications, contact the NTIA/ITS Technical Publications Office at 325 Broadway, Boulder, CO, 80305 Tel. (303) 497-3572 or e-mail info@its.blrdoc.gov.